1
Gold(I) Nitrogen Chemistry

Hanan E. Abdou, Ahmed A. Mohamed, and John P. Fackler Jr

1.1
Introduction

Nitrogen ligands have rarely been used with gold(I) and hardly any chemistry has been described using anionic, bridging nitrogen ligands. Dinuclear gold(I) complexes containing either one or two bridging ligands, such as ylides and thiolates, and their oxidative-addition products have been attracting considerable attention for many years [1, 2]. Gold(I) complexes with N-donor ligands are much less common than those with P-donor ligands. However, the affinity of gold for nitrogen can be increased if a phosphine ligand is attached to gold, because of the efficient π-acceptor nature of the phosphine [2]. Therefore the majority of gold(I) complexes with anionic N-donor ligands (L^-) are complexes of the type R_3PAuL, such as Ph_3PAu(bis (trimethylsilyl)amide) and Ph_3PAu(4-nitro-anilide). Other complexes with L^- corresponding to substituted pyrazoles, imidazoles and benzylimidazoles are also known [2]. The gold(I) amidinate complexes reviewed here are symmetrical with the Au atom bonded to two N atoms. Some work with gold(I) carbeniates (N,C) and benzylimidazolates (N,C) and pyrazolates (N,N) is also included in this review. Gold(III) complexes with nitrogen ligands are covered in Chapter 2 of this book.

Gold(I) with its $[Xe]4f^{14}5d^{10}$ electronic configuration is often described as a soft metal ion [3] and therefore might be expected to have a preference for soft donor ligands such as sulfur and carbon over hard donor ligands such as those bonding through nitrogen or oxygen [4]. For example, when bifunctional ligands with two different donor atoms are used, the gold atom will bind to these ligands through the atom with the higher donor strength according to the sequence [2]: $Si \sim P > C > S > Cl > N > O > F$.

The bifunctional ligands, for example 2-pyridylphophines, thioamides and the 1,1-dicyanoethylene-2,2-dithiolate, are coordinated to gold through the P and S atoms but not N, since P and S atoms are better "soft" donor atoms than N [5]. Therefore, it was generally assumed that gold(I) will not effectively coordinate to a donor nitrogen atom [2]. However, the interesting chemistry of the anionic bridging ligands, amidines, ArNHC(H)NAr, to be described here, does not bear this out.

Gold Chemistry: Applications and Future Directions in the Life Sciences. Edited by Fabian Mohr

ISBN: 978-3-527-32086-8

Cotton's group was able to exploit the amidine ligands for the synthesis of a variety of complexes spanning the transition elements [6]. Previous trials by his group to use the anionic bridging ligand amidines with gold(I) indicated that in the case of $[M_2(ArNC(H)NAr)_2]$ compounds, Ar=-C_6H_4-4-Me and M=Ag, Cu, Au, the stability series [7] must be Cu ~ Ag ≫ Au, since they were unable to isolate a gold compound. The gold amidinate complexes reported here are synthesized in open air at room temperature and are stable at room temperature for several months.

Theoretical studies by Pyykkö in 1998 for $[M_2(NHCHNH)_2]$ systems, M=Cu, Ag, and Au, predicted the M–M distances at the MP2 level [8]. Experimentally, systems containing amidinate ligands were known with Cu and Ag but unknown with Au. The results for the models containing silver and copper are close to the X-ray structures of $[M_2(ArNC(H)NAr)_2]$, Ar=C_6H_4-4-Me and M=Ag, Cu. The Ag–Ag distance is 2.705 and 2.712 Å and the Cu–Cu distance is 2.497 and 2.528 Å at the experimental and theoretical level, Table 1.1. The hypothetical dinuclear gold(I) amidinate compound was calculated to have an Au–Au distance at the MP2 level of 2.728 Å [8]. The dinuclear gold(I) amidinate complex now known proves the predicted Au-Au distance to be rather good.

Only very few examples of gold(II) nitrogen compounds are known. There is only one gold(II) nitrite complex, $Au_2(ylide)_2(NO_2)_2$, reported in the book, Gold Progress in Chemistry, Biochemistry, and Technology, which was synthesized by Fackler and co-workers [2]. The great majority of compounds with gold nitrogen bonds occur with gold in the oxidation states +I and +III with the electronic configuration [Xe] $4f^{14}5d^{10}6s^06p^0$ and [Xe]$4f^{14}5d^86s^06p^0$ respectively [3]. There is a strong tendency for disproportionation from Au(II) to Au(I) and Au(III) in mononuclear complexes [9] because the odd electron in d^9 metal complexes is in the antibonding d_{x2-y2} σ orbital, strongly overlapping with the ligand orbitals (octahedral, tetragonally distorted or square planar). Surprisingly, several gold(II) amidinate complexes have been produced. However, they are dinuclear species. The Au(II) amidinate complexes also have halides or pseudo-halides coordinated to the Au(II) and are stable at room temperature.

Table 1.1 Optimized geometries at MP2 level and selected experimental structural parameters for $[M_2(NHCHNH)_2]$ [8].

System	M-M (Å)	M-N (Å)
$[Au_2(NHCHNH)_2]$	2.728	2.005
$[Ag_2(NHCHNH)_2]$	2.712	2.043
$[Cu_2(NHCHNH)_2]$	2.528	1.834
Experimental structural parameters for $[M_2(NHCHNH)_2]$, M = Ag and Cu		
$[Cu_2(ArNC(H)NAr)_2]$, Ar = C_6H_4-4-Me	2.497	1.886
$[Ag_2(ArNC(H)NAr)_2]$, Ar = C_6H_4-4-Me	2.705	2.116

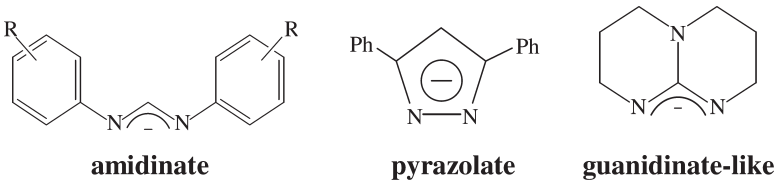

Figure 1.1 Some of the nitrogen ligands discussed in this review.

The anionic amidinate ligands, Figure 1.1, are known for their remarkable ability to bridge between the metal ions, facilitating the formation of short metal–metal distances and for their flexible coordination modes, leading to various molecular arrangements [10]. The use of these amidinate ligands in the coordination chemistry of the transition metals has produced complexes with extraordinarily short M–M distances [6]. These short distances are due, at least in part, to the ability of the amidinate anion to delocalize the negative charge while strongly donating sigma electron density to the metal atoms, supporting bond formation [11]. Previous studies have shown that the amidinate ligands form dinuclear Ag(I) and Cu(I) complexes [7, 12, 13]. Placing alkyl and aryl substituents on the amidinate NCN carbon atom influences the formation of tetranuclear and trinuclear structural motifs with Ag(I) [14]. Clearly the substituents play a role in determining the nuclearity and molecular arrangement of the complexes.

The nitrogen ligand chemistry with pyrazolate ligands, Figure 1.1, has produced mainly trinuclear complexes of group 11 with the structure, $[M(\mu\text{-}3,5\text{-}Ph_2Pz)]_3$, M=Cu(I), Ag(I), Au(I). The hexanuclear gold complex $[Au(\mu\text{-}3,5\text{-}Ph_2Pz)]_6$ has also been obtained, although in low yield [15]. Tetranuclear gold(I) pyrazolates were isolated only with a 3,5-di-isobutyl substituted pyrazolate [16]. The guanidinate-type anion ligand hpp (1,3,4,6,7,8-hexahydro-H-pyrimido[1,2-a]pyrimidine), Figure 1.1, forms complexes with extra short M–M bonding distances and stabilizes metals in high oxidation states [6]. Gold(I) and gold(II) complexes were isolated with the hpp ligand [17, 18].

1.2
Tetra-, Tri-, and Dinuclear Gold(I) Amidinate Complexes

The structural arrangement of group 11 amidinate complexes is determined by the substituents on the amidinate aryl groups as well as on the NCN carbon [14, 19]. The electronic vs. steric effect of the substituents on the molecular arrangement of gold(I) amidinate complexes have been studied in detail in the Fackler laboratory.

A series of symmetrical diaryl substituted amidinate ligands, ArNH(CH)NAr, has been synthesized, Figure 1.2. The substituents on the NCN aryl group vary from electron withdrawing groups such as $\text{-}C_6F_5$, $3\text{-}CF_3\text{-}C_6H_4$, $3,5\text{-}Cl\text{-}C_6H_3$ to donating groups such as $4\text{-}OMe\text{-}C_6H_4$, $4\text{-}Me\text{-}C_6H_4$, $\text{-}C_{10}H_7$. Ligands with sterically bulky groups in the ortho positions such as $2,6\text{-}Me_2\text{-}C_6H_3$ as well as on the NCN carbon, NC(Me)N and NC(Ph)N, have also been prepared. The amidine ligands are readily

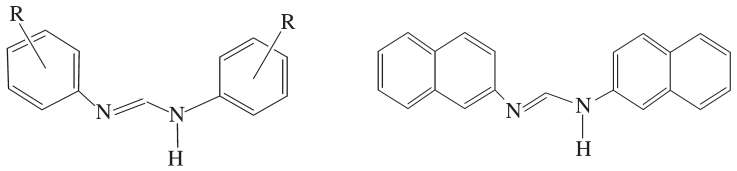

R = 4-Me, 4-OMe, 3-CF_3, 3,5-Cl, 2,3,4,5,6-pentafluoro

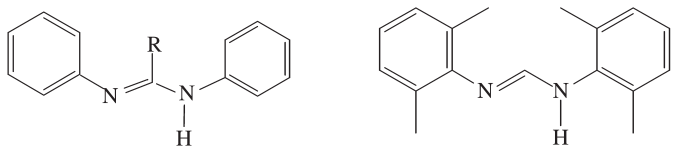

R = -CH_3, -C_6H_5

Figure 1.2 Amidine ligands used in the synthesis of terta-, tri-, and dinuclear gold complexes.

synthesized using modified literature procedures [14, 20]. The aniline derivative and triethylorthoformate (orthoester) are mixed and the reaction mixture heated to 140–160 °C to form the imido ester which later forms the amidine ligand, Figure 1.3.

Tetranuclear gold(I) amidinate complexes are synthesized by the reaction of Au(THT)Cl with the potassium or sodium salt of the amidinate ligand in THF, Figure 1.4. Syntheses involving various substituted amidinates resulted in tetranuclear gold(I) clusters, $[Au_4(ArNC(H)NAr)_4]$. The C-functionalized substituted amidine ligands, ArNC(Ph)NHAr and ArNC(Me)NHAr, Ar=-C_6H_5, were synthesized and reacted with Au(THT)Cl after deprotonation. Only tetranuclear clusters were isolated.

In each tetranuclear Au(I) aryl amidinate complex studied, $[Au_4(ArNC(H)NAr)_4]$, the NC bond length in NCN is ~1.3 Å, indicating delocalization across the amidinate bridge. The four gold atoms are located at the corners of a rhomboid with the amidinate ligands bridged above and below the near plane of the four gold(I) atoms, Figures 1.5 and 1.6. The average Au · · · Au distance is ~3.0 Å, typical of Au(I) · · · Au(I)

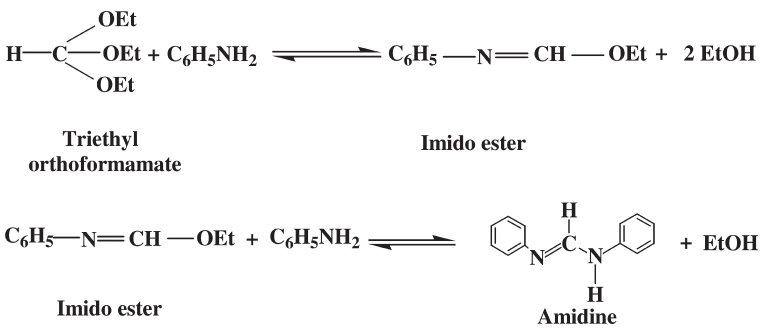

Figure 1.3 Synthesis of the amidine ligands.

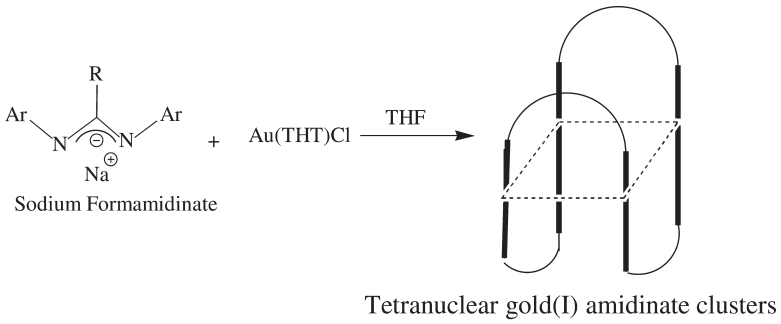

R = H, Ar = C_6H_4-4-Me, C_6H_4-4-OMe, C_6H_3-3,5-Cl, C_6H_4-3-CF_3, -$C_{10}H_7$, -C_6F_5
R = -C_6H_5, Ar = -C_6H_5
R = -CH_3, Ar = C_6H_5

Figure 1.4 Schematic representation of the reaction between amidinate ligands and Au(THT)Cl.

aurophilic interactions. The four gold atoms are arranged in a near square (Au · · · Au · · · Au = 87–92°) in the tetranuclear structure [Au_4(ArNC(H)NAr)$_4$], Ar=-C_6F_5. The packing diagram shows weak F · · · F (∼2.44 Å), Au · · · F (∼3.14 Å intramolecular), and Au · · · F (∼3.51 Å, intermolecular) interactions. Figures 1.7 and 1.8 are thermal ellipsoid plots of [Au_4(ArNC(Ph)NAr)$_4$] and [Au_4(ArNC(CH_3)NAr)$_4$], Ar= -C_6H_5. The average Au · · · Au distance is 2.94 Å, typical of Au(I) · · · Au(I) aurophilic interactions. The gold atoms are arranged in a near square (Au · · · Au · · · Au = 88–91°)

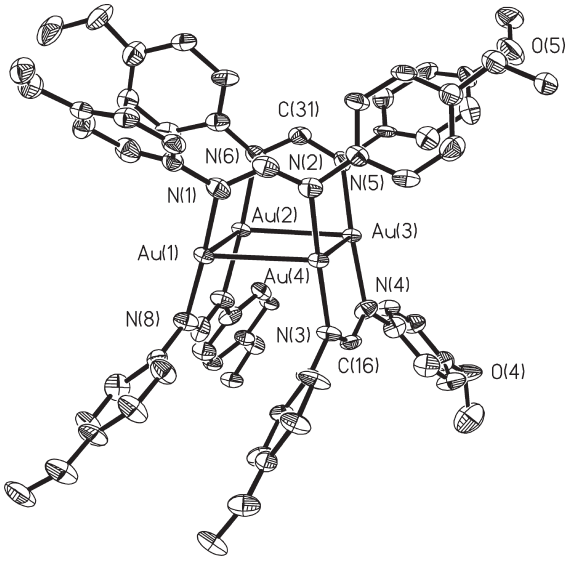

Figure 1.5 Thermal ellipsoid plot of [Au_4(ArNC(H)NAr)$_4$], Ar = 4-OMe-C_6H_4.

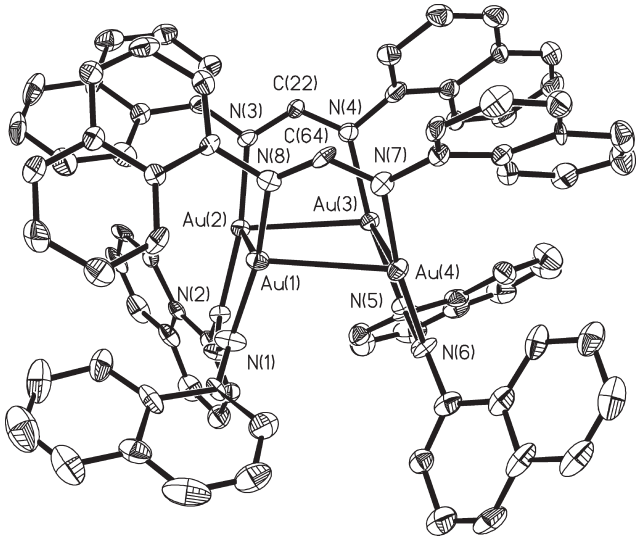

Figure 1.6 Thermal ellipsoid plot of $[Au_4(ArNC(H)NAr)_4]$, $Ar = C_{10}H_7$.

in $[Au_4(C_6H_5NC(CH_3)NC_6H_5)_4]$ and a distorted square ($Au \cdots Au \cdots Au = 82–97^\circ$) in $[Au_4(C_6H_5NC(Ph)NC_6H_5)_4]$.

Table 1.2 gives the $Au \cdots Au$ distances, and $Au \cdots Au \cdots Au$ and N–Au–N angles for several homobridged tetranuclear Au(I) complexes and tetranuclear gold amidinate complexes. Similar structural arrangements have been found in the tetrameric 1,3-diphenyltriazenidogold(I) complex, $[Au(PhNNNPh)]_4$ ($Au \cdots Au = 2.85$ Å) [21],

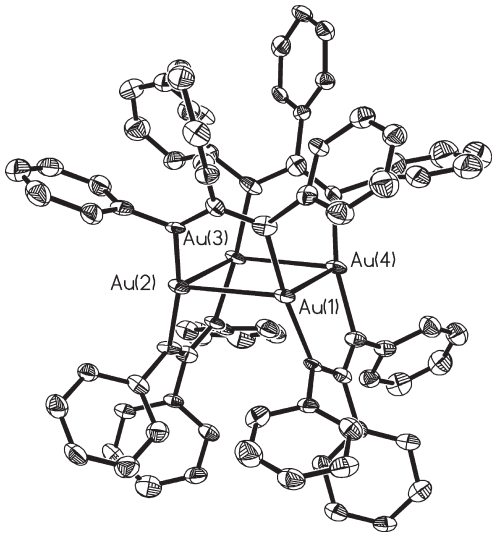

Figure 1.7 Thermal ellipsoid plot of $[Au_4(C_6H_5NC(Ph)NC_6H_5)_4]$.

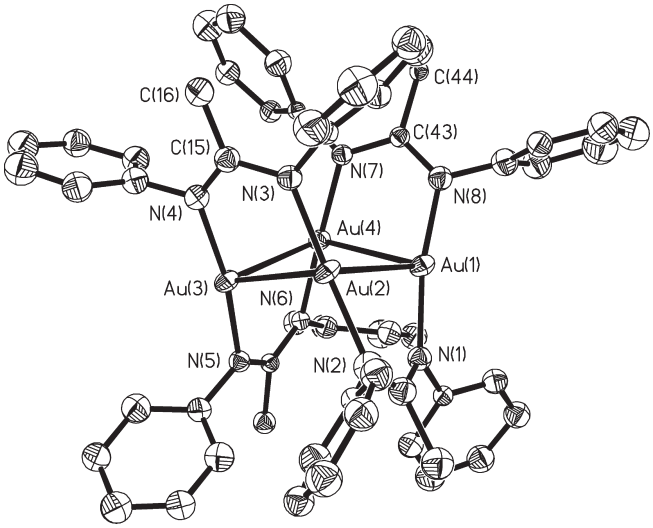

Figure 1.8 Thermal ellipsoid plot of $[Au_4(C_6H_5NC(CH_3)NC_6H_5)_4]$.

$[Au_4(CH_3CS_2)_4]$ (Au · · · Au = 3.01 Å) [22] and the tetranuclear gold pyrazolate complex $[Au(3,5\text{-t-Bu-pz})]_4$ (Au · · · Au = 3.11 Å) [16]. The Au(I) atoms bridged by the more flexible amidinate ligands show shorter Au · · · Au distances than those bridged by the rigid pyrazolate ligands (i.e., 2.9 Å versus 3.1 Å) [13].

Using sterically bulky groups in the ortho positions of the phenyl rings in ArNC(H)NHAr, such as Ar = 2,6-Me_2-C_6H_3, led to formation of dinuclear and trinuclear complexes. This suggests that steric factors can prevent the formation

Table 1.2 Average Au · · · Au distances (Å) and Au · · · Au · · · Au angles (°) of tetranuclear gold(I) amidinate and related clusters.

Complex	Au · · · Au	Au(1) · · · Au(2) · · · Au(3)	N-Au-N	Ref
$[Au(PhNNNPh)]_4$	2.85	89.92	176	[21]
$[Au(CH_3CS_2)]_4$	3.01	89.95	167	[22]
$[Au(3,5\text{-t-Bu-pz})]_4$	3.11		175	[16]
Amidinate clusters $[Au_4(ArNC(H)NAr)_4]$, Ar =				
C_6H_4-4-OMe	2.94	70.87, 109.12	174	[19]
C_6H_3-3,5-Cl	2.91	88.30, 91.53	177	[19]
C_6H_4-4-Me	3.03	63.59, 116.4	172	[19]
$C_{10}H_7$	2.98	68.52, 110.88	170	[19]
C_6F_5	2.96	92.3, 87.5	169	[19]
C_6H_4-3-CF_3	2.92	84.6, 95.3	176	[19]
Amidinate clusters $[Au_4(PhNC(R)NPh)_4]$, R=				
C_6H_5	2.94	82.86, 97.66	173	[19]
CH_3	2.93	88.47, 91.14	168	[19]

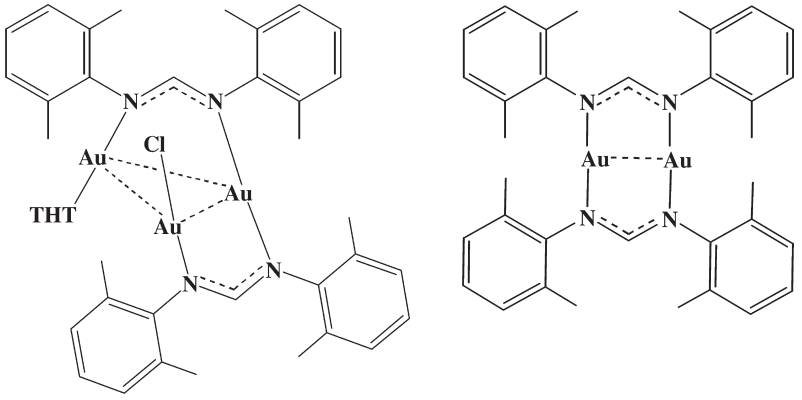

Figure 1.9 Structure of the trinuclear and dinuclear gold amidinate complexes.

of tetranuclear gold(I) amidinates, Figure 1.9 [23]. Models show that formation of the tetranuclear species is blocked by ligand-ligand interactions. Previous work indicated the formation of a dinuclear product, Au · · · Au = 2.646 Å , when Me_3Si was bonded to the N atoms, $\{Au_2[(Me_3SiN)_2C(Ph)]_2\}$ [4]. The formation of the dinuclear Au(II) guanidinate complex $[Au_2(hpp)_2Cl_2]$ also implicates the possible presence of a dinuclear Au(I) species with this sterically uncrowded ligand [17, 18].

The trinuclear species $[Au_3(2,6\text{-}Me_2\text{-form})_2(THT)Cl]$ and the dinuclear $[Au_2(2,6\text{-}Me_2Ph\text{-form})_2]$ were isolated by the reaction of the potassium salt of the corresponding amidinate ligand with (THT)AuCl, Figure 1.10. The structure of the trinuclear gold complex shows a short Au · · · Au distance of ∼3.01 Å and a longer Au · · · Au distance of 3.66 Å, Figure 1.11. The Au · · · Au distance in the dinuclear complex $[Au_2(2,6\text{-}Me_2Ph\text{-form})_2]$ is 2.711(3) Å, and the N-Au-N angle is 170.2(3)°. To our knowledge, the only other example of a symmetrically bridged dinuclear gold(I) nitrogen complex is $\{Au_2[(Me_3SiN)_2C(Ph)]_2\}$, which has an Au · · · Au distance of 2.646 Å [24]. The Au · · · Au distance in $[Au_2(2,6\text{-}Me_2Ph\text{-form})_2]$ is 2.711 Å, Figure 1.12, close to the distance suggested by Pyykkö [8] for the $[Au_2(NHCHNH)_2]$. This is shorter than in the xanthate $[Au_2(^nBu\text{-xanthate})_2$ (2.849 Å) [25], the dithiophosphinate $[AuS_2PPh_2]_2$ (3.085 Å) [26], ylide $[Au(CH_2)_2PPh_2]_2$ (2.977 Å) [27], and dithiophosphonate $[AuS_2PPh(OEt)]_2$ (3.042 Å) [28], but somewhat closer to the observed Au · · · Au distances in the dithiolates $[PPN]_2[Au_2(\mu^2\text{-}\eta^2\text{-}CS_3)_2]$ (2.799 Å) [29], $[n\text{-}Bu_4N][Au(S_2C{=}C(CN)_2]_2$ (2.796 Å) [30], and $[Au(S_2C{-}N(C_5H_{11})_2)]_2$ (2.769 Å) [31].

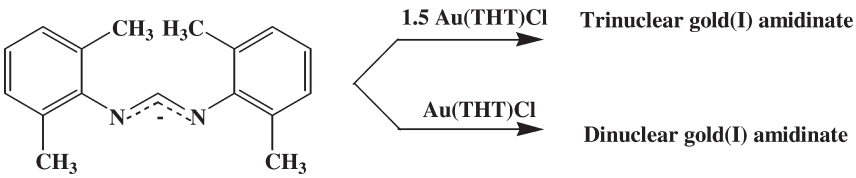

2,6-dimethyl amidinate

Figure 1.10 Synthesis of dinuclear and trinuclear gold(I) amidinates.

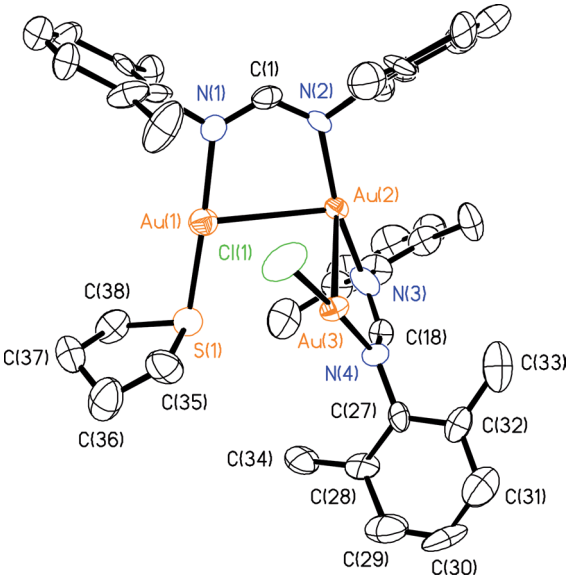

Figure 1.11 Thermal ellipsoid plot of $[Au_3(2,6\text{-}Me_2Ph\text{-}form)_2(THT)Cl]$.

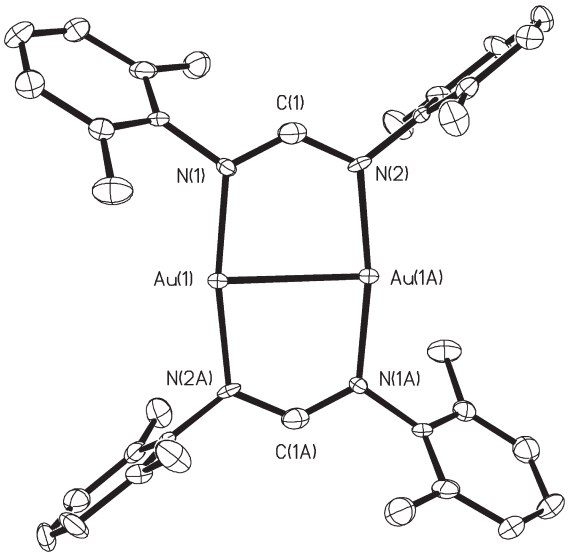

Figure 1.12 Thermal ellipsoid plot of $[Au_2(2,6\text{-}Me_2Ph\text{-}form)_2]$.

1.3
Oxidative-Addition Reactions to the Dinuclear Gold(I) Amidinate Complex

Oxidative-addition reactions have been widely studied with bridged dinuclear metal complexes [1, 2, 5, 32]. Earlier work with the ylides and sulfur bonded ligands

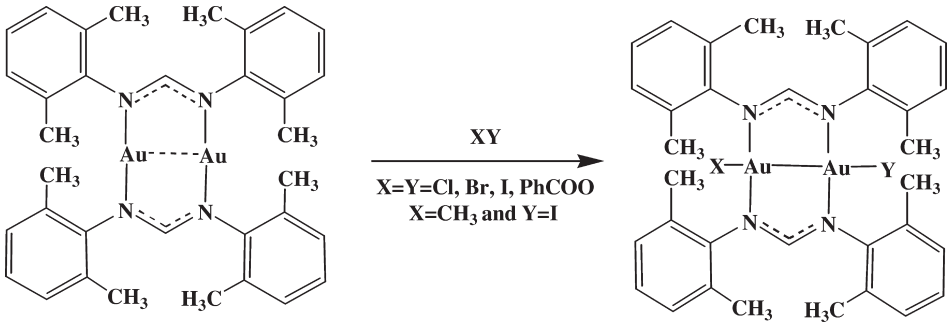

Figure 1.13 Synthesis of gold(II) amidinate complexes by oxidative-addition to the dinuclear gold(I) amidinate.

(*vide infra*) has led to the formation of many Au(II)-Au(II) bonded complexes. No stable organometallic alkyl halide addition products of dinuclear Au(I) complexes have been characterized with ligands other than the ylides [32]. Oxidative-addition reactions to the dinuclear gold(I) amidinate complex, $[Au_2(2,6\text{-}Me_2Ph\text{-}form)_2]$, result in the formation of Au(II) complexes. The Au(II) amidinate complexes are the first gold(II) species isolated with nitrogen ligands [23]. The complexes are stable at room temperature. Various reagents such as Cl_2, Br_2, I_2, benzoyl peroxide and CH_3I add to the dinuclear gold(I) amidinate complex to form oxidative-addition gold(II) products, $[Au_2XY(2,6\text{-}Me_2Ph\text{-}form)_2]$, Figure 1.13 [23, 33, 34]. The methyl iodide addition product is the only organometallic Au(II) species formed to date with amidinate ligands [33].

The reaction of the dinuclear complex, $[Au_2(2,6\text{-}Me_2Ph\text{-}form)_2]$, with the halogenated solvents, CH_2X_2, XCH_2CH_2X, CX_4 (X=Cl, Br, I) also forms Au(II) products. With the iodide derivatives the reaction occurs at the time of mixing. The analogous reactions with chloride and bromide derivatives take approximately 2–3 days, and 7 days with CH_2Cl_2 in order to oxidize all the Au(I) material. A crystalline product in which there are equal amounts of oxidized and unoxidized complexes in the same unit cell, $[Au_2(2,6\text{-}Me_2Ph\text{-}form)_2X_2][Au_2(2,6\text{-}Me_2Ph\text{-}form)_2]$, X=Cl and X=Br, Figure 1.14, is isolated when the reaction is stopped after 3–4 h of stirring. In the reaction of the haloalkyls CH_nX_m, the qualitative order of reactivity with the dinuclear

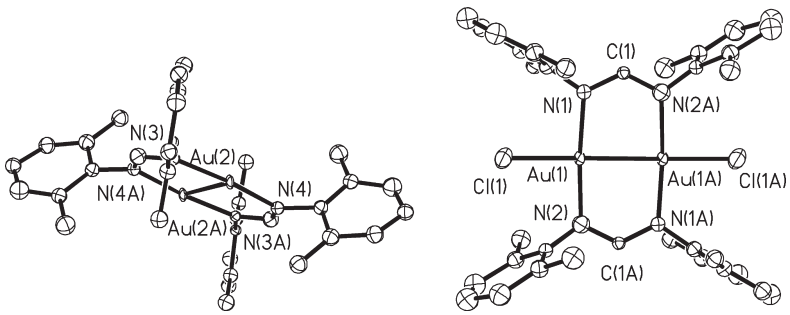

Figure 1.14 Thermal ellipsoid plot of $[Au_2(2,6\text{-}Me_2Ph\text{-}form)_2Cl_2][Au_2(2,6\text{-}Me_2Ph\text{-}form)_2]$.

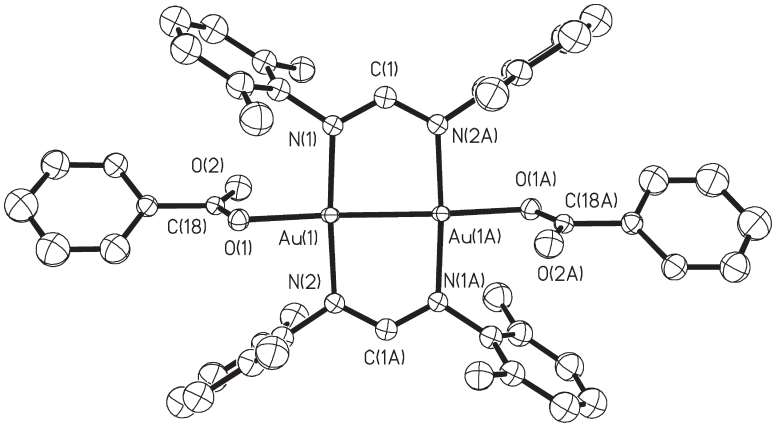

Figure 1.15 Thermal ellipsoid plot of $[Au_2(2,6\text{-}Me_2Ph\text{-}form)_2(PhCO)_2]$.

gold complex (I > Br > Cl) follows inversely the order of carbon-halogen bond dissociation energy, C–Cl > C–Br > C–I.

The oxidative-addition of benzoyl peroxide, $(PhCOO)_2$, leads to the isolation of the first stable dinuclear gold(II) nitrogen complex also possessing Au–O bonds, $[Au_2(2,6\text{-}Me_2Ph\text{-}form)_2(PhCO_2)_2]$ [34]. An analogous ylide complex, $[Au_2((CH_2)_2PPh_2)_2(PhCO_2)_2]$ is known [33]. The benzoate amidinate product $[Au_2(2,6\text{-}Me_2Ph\text{-}form)_2(PhCO)_2]$ was obtained, Figure 1.15, by adding an equivalent amount of benzoyl peroxide to a toluene solution of the dinuclear Au(I) amidinate. Infra-red spectroscopic studies of the gold(II) benzoate complex show two intense bands at 1628 and 1578 cm^{-1} due to ν(C=O) and at 1320–1295 cm^{-1} due to ν(C−O) frequencies. The separation between the two bands is ∼300 cm^{-1}, typical of unidentate benzoate bonding, a "pseudo ester" character. The bonding of the benzoates to the dinuclear gold(II) amidinate is similar to the unidentate bonding observed in the ylide complexes, which adopt an *anti* geometry [2, 35].

The oxidative-addition of benzoyl peroxide to the dinuclear gold(I) ylide complex formed a gold(II) complex with the shortest Au · · · Au distance observed, 2.56–2.58 Å [2,35], for the dinuclear Au(II) ylide complexes, Table 1.3. Similarly, the Au · · · Au distance in the oxidized product $[Au_2(2,6\text{-}Me_2Ph\text{-}form)_2(PhCO)_2]$, 2.48 Å [34], is the shortest Au · · · Au distance in the Au(II) amidinate complexes. The short Au · · · Au distance in these complexes is due to the weak *trans*-directing and sigma covalent bonding ability of the carboxylate ligands to gold(II) compared with the halides [34].

A facile replacement of the benzoate groups in $[Au_2(2,6\text{-}Me_2Ph\text{-}form)_2(PhCOO)_2]$ by chloride or bromide is achieved by adding equivalent amounts of $PhICl_2$ or $[Bu_4N]Br$, Figure 1.16. The replacement of the bromide in $[Au_2(2,6\text{-}Me_2Ph\text{-}form)_2Br_2]$ by chloride is achieved by adding 1 mol of $PhICl_2$ to 1 mol in polar solvent such as CH_3CN.

The X-ray crystallography of the gold(II) amidinate complexes shows a decrease in the Au · · · Au distance from 2.71 Å in the starting dinuclear complex to 2.51–2.57 Å in the oxidized species. The Au–X distances are Au–Cl = 2.36 Å, Figure 1.17, Au–Br = 2.47 Å, and Au–I = 2.68 Å, Figure 1.18. The Au–N distances decreases from

Table 1.3 Dinuclear Au(II) ylide and amidinate complexes characterized by X-ray studies.

Complex	d($Au^{II}\cdots Au^{II}$)	d(Au-X)	d(Au-R)	Ref
$[ClAu(CH_2PPh_2CH_2)_2AuCl]$	2.600(1)	2.388(8)		[9]
$[BrAu(CH_2PPh_2CH_2)_2AuBr]$	2.614(1)	2.516(1)		[9]
$[IAu(CH_2PPh_2CH_2)_2AuI]$	2.650	2.693(8)		[9]
$[(CH_3)Au(CH_2PPh_2CH_2)_2AuI]$	2.695(4)			[9]
$[(CH_3)Au(CH_2PMe_2CH_2)_2AuI]$	2.695(4)	2.894(5)	2.13(5)	[9]
$[PhCO_2Au(CH_2PPh_2CH_2)_2AuO_2CPh]$	2.561(2)	2.117(13)		[9]
$[ClAu(2,6\text{-}Me_2Ph\text{-}form)_2AuCl]$	2.517(7)	2.356(2)		[34]
$[BrAu(2,6\text{-}Me_2Ph\text{-}form)_2AuBr]$	2.525(15)	2.470(2)		[34]
$[IAu(2,6\text{-}Me_2Ph\text{-}form)_2AuI]$	2.579(4)	2.682(4)		[346]
$[(CH_3)Au_2(2,6\text{-}Me_2Ph\text{-}form)_2AuI]$	2.529(11)	2.50	2.12	[33, 34]
$[PhCO_2Au(2,6\text{-}Me_2Ph\text{-}form)_2AuO_2CPh]$	2.489(10)	2.045(8)		[34]

2.035(7) Å in the dinuclear complex to 2.00–2.004 Å in the oxidative-addition products. The Au atoms have a nearly square-planer coordination geometry.

The reaction of methyl iodide, CH_3I, with $[Au_2(2,6\text{-}Me_2Ph\text{-}form)_2]$ in ether generates $[CH_3Au(2,6\text{-}Me_2Ph\text{-}form)_2AuI]$ in quantitative yield under nitrogen at 0 °C, in the absence of light [33, 34]. While the Au(II) atoms and the amidinate ligand atoms refine well, unfortunately, the structure has a disorder in the CH_3 and iodide positions since the spatial volume occupied by CH_3 and I is approximately identical. As a result their positions remain uncertain with regard to their exact distances from the Au(II) atoms. The Au–CH_3 and Au–I distances appear to be 2.12 Å and 2.50 Å, while in the dinuclear gold(I) ylide, $[(CH_3)Au((CH_2)2PMe_2)_2AuI]$, the Au–$CH_3$ and Au–I distances are 2.13(5) and 2.894(5) Å, respectively, and the Au(II) –Au(II) distance is 2.695(4) Å [9]. Surprisingly, the Au–I distance in the Au(II) amidinate complex appears to be shorter than found in the ylide, $[IAu((CH_2)_2PMe_2)_2AuI]$.

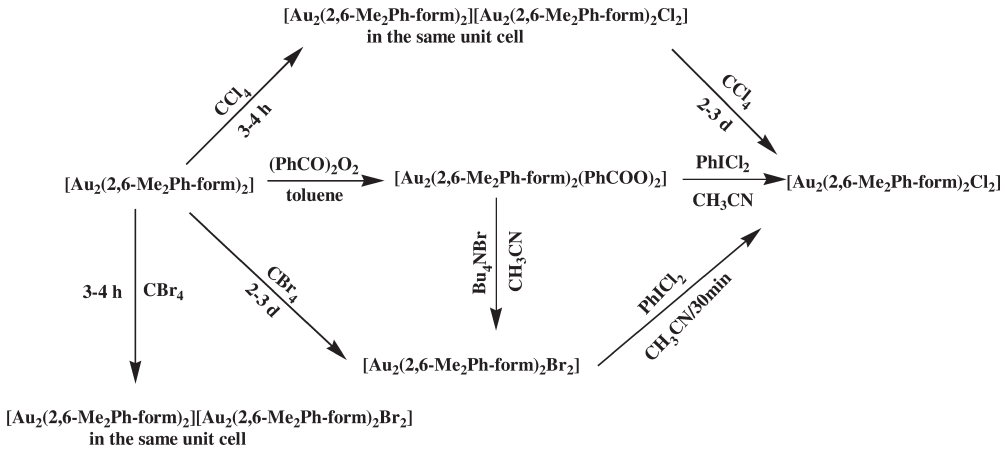

Figure 1.16 Schematic representation of the replacement reactions of $[Au_2(2,6\text{-}Me_2Ph\text{-}form)_2]$.

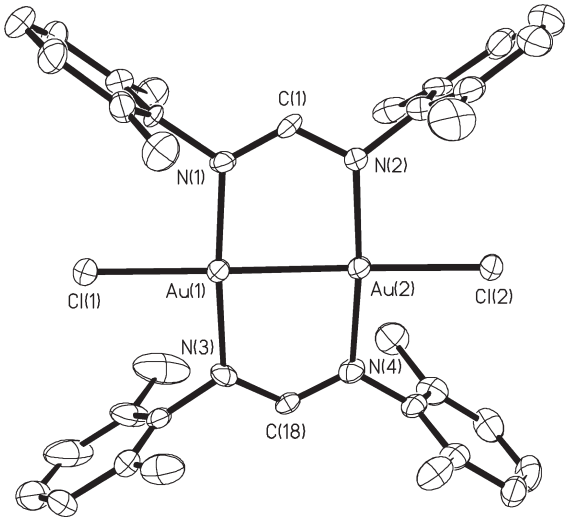

Figure 1.17 Thermal ellipsoid plot of $[Au_2(2,6\text{-}Me_2Ph\text{-}form)_2Cl_2]$.

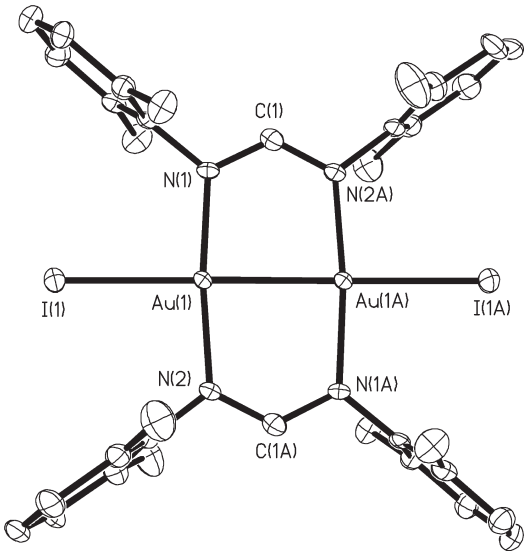

Figure 1.18 Thermal ellipsoid plot of $[Au_2(2,6\text{-}Me_2Ph\text{-}form)_2I_2]$.

1.4
Mercury(II) Cyanide Coordination Polymer

The reaction of the dinuclear gold(I) amidinate complex, $[Au_2(2,6\text{-}Me_2Ph\text{-}form)_2]$, with $Hg(CN)_2$ (1 : 2 stoichiometry) in THF forms a 2D coordination polymer, $[Au_2(2,6\text{-}Me_2Ph\text{-}form)_2]\cdot 2Hg(CN)_2\cdot 2THF$, not the expected oxidative-addition product of the type formed with the ylides. White crystals and a yellow powder are formed.

The white crystals change to yellow powder upon grinding, presumably with loss of THF and possibly some AuCN formation. Thermal gravimetric analysis of $[Au_2(2,6\text{-}Me_2Ph\text{-}form)_2]\cdot 2Hg(CN)_2\cdot 2THF$ showed the release of THF gradually at >120 °C followed by decomposition at >200 °C. The powder diffraction pattern of the yellow residue after heating above 265 °C showed a pattern typical of AuCN (IR 2236 cm^{-1}) as confirmed by comparison with the powder diffraction pattern of a sample of AuCN obtained from the Aldrich Chemical Co.

The behavior of $Hg(CN)_2$ toward the dinuclear gold(I) amidinate complexes requires comment. In the case of the dinuclear gold(I) ylide, oxidation of the Au(I) to Au(II) resulted in the formation of a reduced mercury(0) product, Figure 1.19(a) [36]. In the mercury(II) cyanide reaction with the dinuclear gold(I) dithiophosphinate, Figure 1.19(b), the stability of the gold(I)-carbon bond compared

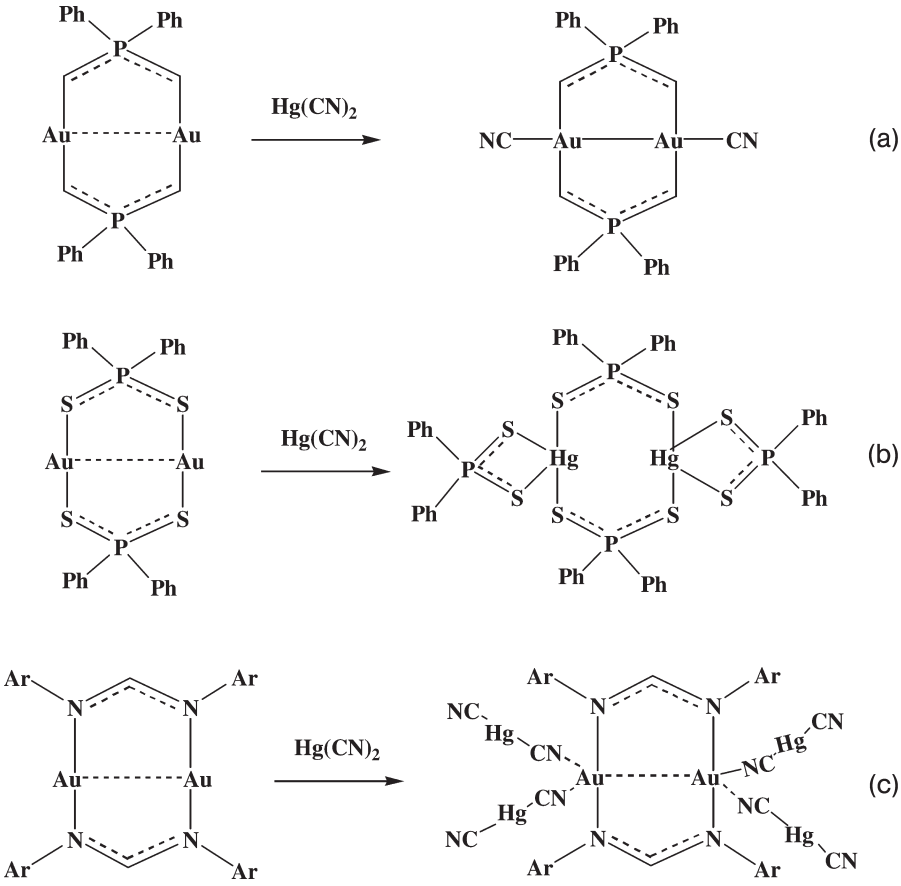

Figure 1.19 Schematic representation of the reactions between $Hg(CN)_2$ and the (a) dinuclear gold(I) ylide with loss of Hg(0), (b) dinuclear gold(I) dithiophosphinate with los of AuCN, and with (c) dinuclear Au(I) 2,6-Me_2formamidinate complexes.

with that of mercury(II)-carbon bond and the strength of the Hg(II)–S bonds compared with the labile Au(I)–S bonds appear to lead to the metathesis products observed. With the adduct to the amidinate ligand complex, Figure 1.19(c), the cyanide IR stretching frequency shifts from 2192 cm^{-1} in $Hg(CN)_2$ to ~2147 cm^{-1}, a value very near to the CN stretching frequency found (2145 cm^{-1}) in the dinuclear Au(II) ylide dicyanide [37]. However, the oxidation of the dinuclear Au(I) amidinate by the $Hg(CN)_2$ is much more difficult than the oxidation of the dinuclear Au(I) ylide. Cyclic voltammetric studies bear this out (*vide infra*) [38].

The differences observed in the chemistry of these dinuclear gold(I) amidinate complexes compared with dinuclear gold(I) complexes with sulfur and carbon ligands may be understood by examining their respective highest occupied molecular orbital (HOMO)s and lowest unoccupied molecular orbital (LUMO)s of the species. In the ylide complexes the HOMO is a metal-metal σ^* antibonding orbital, and the LUMO is a bonding σ orbital directed along the metal-metal axis. In the dinuclear gold(I) amidinates the HOMO is δ^* with regard to the π orbitals of the N ligands [39] and the LUMO is also largely ligand based.

Gold(I) ylides are oxidized in 0.1 M $[Bu_4N]BF_4$/THF at low potentials of $+0.11$ and $+0.23$ V vs. Ag/AgCl (quasi-reversible). The dinuclear amidinate oxidizes under the same conditions at $+1.24$ V vs. Ag/AgCl (reversible). These large differences in chemical character of the dinuclear gold(I) complexes appear to explain the widely different behavior of these compounds and especially toward the reaction with mercury cyanide.

The adduct formation of $Hg(CN)_2$ to the $[Au_2(2,6\text{-}Me_2Ph\text{-}form)_2]$ increases the Au···Au distance from 2.7 Å in the dinuclear complex to 2.9 Å in the adduct, Figure 1.20. The gold centers are coordinated by four nitrogen atoms with Au–N distances in the range 2.09–2.51 Å. The N-Au-N angles associated with the amidinate ligands decreased from ~170° in the dinuclear starting material to ~161°. The N-Au-N angles are in the range 95–100° (angles from the cyanide groups). The 2D lattice contains two THF solvent molecules in the large cavities (~10.2 × 13.7 Å), Figure 1.20(b). The Hg–O distance is ~4.33 Å indicating that the interaction between the Hg centers and THF is not significant.

1.5
Formation of Mixed-Ligand Tetranuclear Gold(I) Nitrogen Clusters

Density functional theory (DFT) modeling calculations show that a dinuclear gold(I) amidinate complex is less stable than the tetranuclear gold(I) amidinate cluster, $[Au_4(HNC(H)NH)_4]$. However, replacing C by Si in the backbone reduces ring strain and makes the energies similar, Figures 1.21 and 1.22 [39].

Attempts to introduce less bulky anionic ligands to the dinuclear complex $[Au_2(2,6\text{-}Me_2Ph\text{-}form)_2]$ cause the dinuclear gold(I) amidinate complex to rearrange and form tetranuclear gold(I) amidinate complexes [40]. The ligand exchange of the sterically bulky ligand, 2,6-Me_2Ph-form, in the dinuclear gold(I) amidinate complex with less bulky anionic ligands such as $[ArNC(H)NAr]^-$, Ar=C_6H_4-4-Me, Ar=C_6H_4-4-OMe,

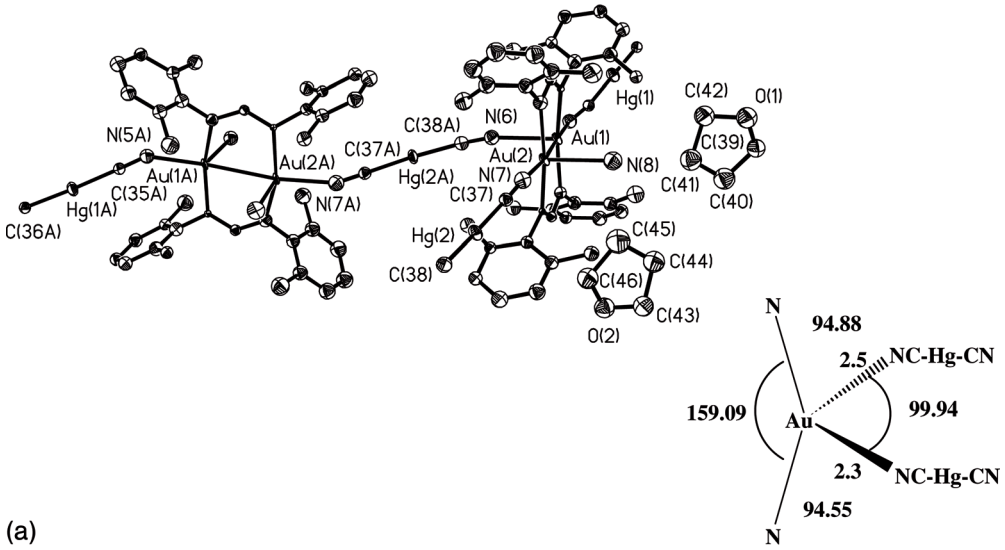

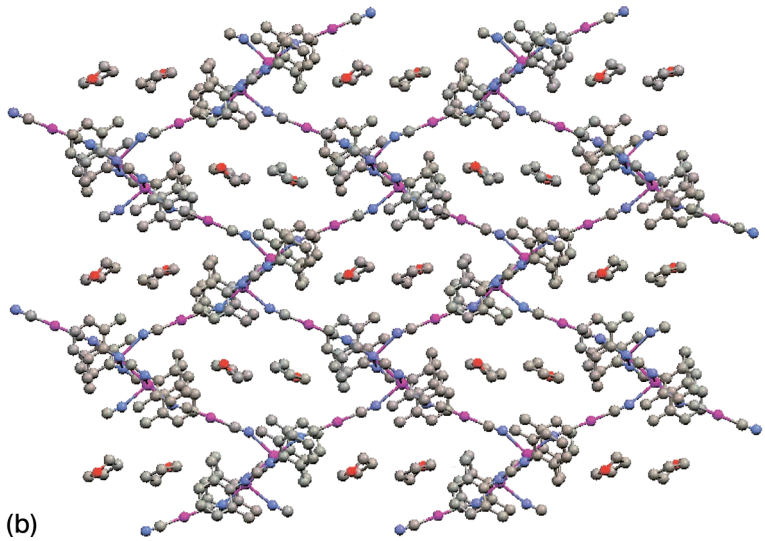

Figure 1.20 (a) Thermal ellipsoid plot and bond distances and angles of $[Au_2(2,6\text{-}Me_2Ph\text{-}form)_2].2Hg(CN)_2{\cdot}2THF$. (b) 2D of $[Au_2(2,6\text{-}Me_2Ph\text{-}form)_2].2Hg(CN)_2{\cdot}2THF$ showing the THF solvent in the voids.

and 3,5-diphenylpyrazolate, to form mixed-ligand species provides a facile procedure for the synthesis of mixed-ligand complexes along with the increased nuclearity, Figure 1.23. Tetranuclear gold(I) complexes with amidinate and pyrazolate ligands can be formed, such as $[Au_4(3,5\text{-}Ph_2pz)_2(2,6\text{-}Me_2Ph\text{-}form)_2]$ and $[Au_4(3,5\text{-}Ph_2pz)_3(2,6\text{-}Me_2Ph\text{-}form)]$. This result was extended to the synthesis of tetranuclear

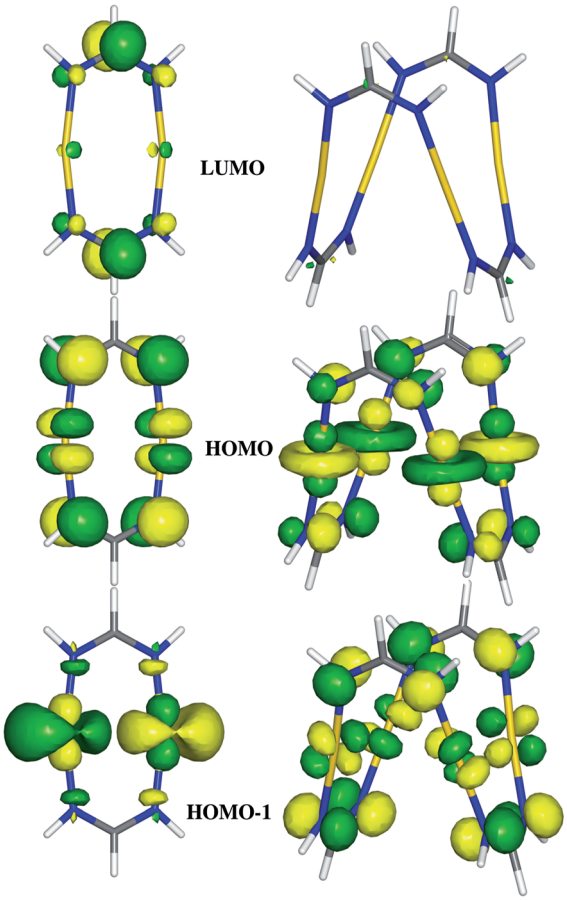

Figure 1.21 HOMO and LUMO of the dinuclear and tetranuclear gold amidinate species.

mixed-metal Au–Ag complexes with pyrazolate and amidinate ligands [Au_2(3,5-Ph_2pz)$_2$ Ag_2(2,6-Me_2Ph-form)$_2$] [40]. This complex is the only tetranuclear amidinate complex observed with the two bulky amidinate ligands facing each other. Apparently, the long Au $\cdots$ Ag distances, $\sim$3.3 Å, allow the bulky amidinate ligands to be in this *syn* arrangement.

Reacting the amidinate salt, K[4-MePh-form], with the dinuclear gold(I) complex, [Au_2(2,6-Me_2Ph-form)$_2$], in a 1 : 1 stoichiometry in THF forms the dinuclear-tetranuclear complex [Au_2(2,6-Me_2Ph-form)$_2$][Au_4(4-MePh-form)$_4$]·2THF, Figure 1.24, with one tetranuclear and one dinuclear molecule in the same unit cell. Adjusting the reaction ratio to 2 : 1 formed the tetranuclear complex [Au_4(4-MePh-form)$_4$].

The reaction of the diphenylpyrazolate salt, Na[3,5-Ph_2pz], with the dinuclear gold(I) complex [Au_2(2,6-Me_2Ph-form)$_2$] in a 1 : 1 stoichiometric ratio resulted in the formation of two tetranuclear products, observed as blocks, [Au_4(3,5-Ph_2pz)$_2$ (2,6-Me_2Ph-form)$_2$]·2THF, Figure 1.25, and as needles, [Au_4(3,5-Ph_2pz)$_3$(2,6-Me_2Ph-form)]·THF, Figure 1.26. Adjusting the reaction ratio to 1.5 : 1 resulted in the

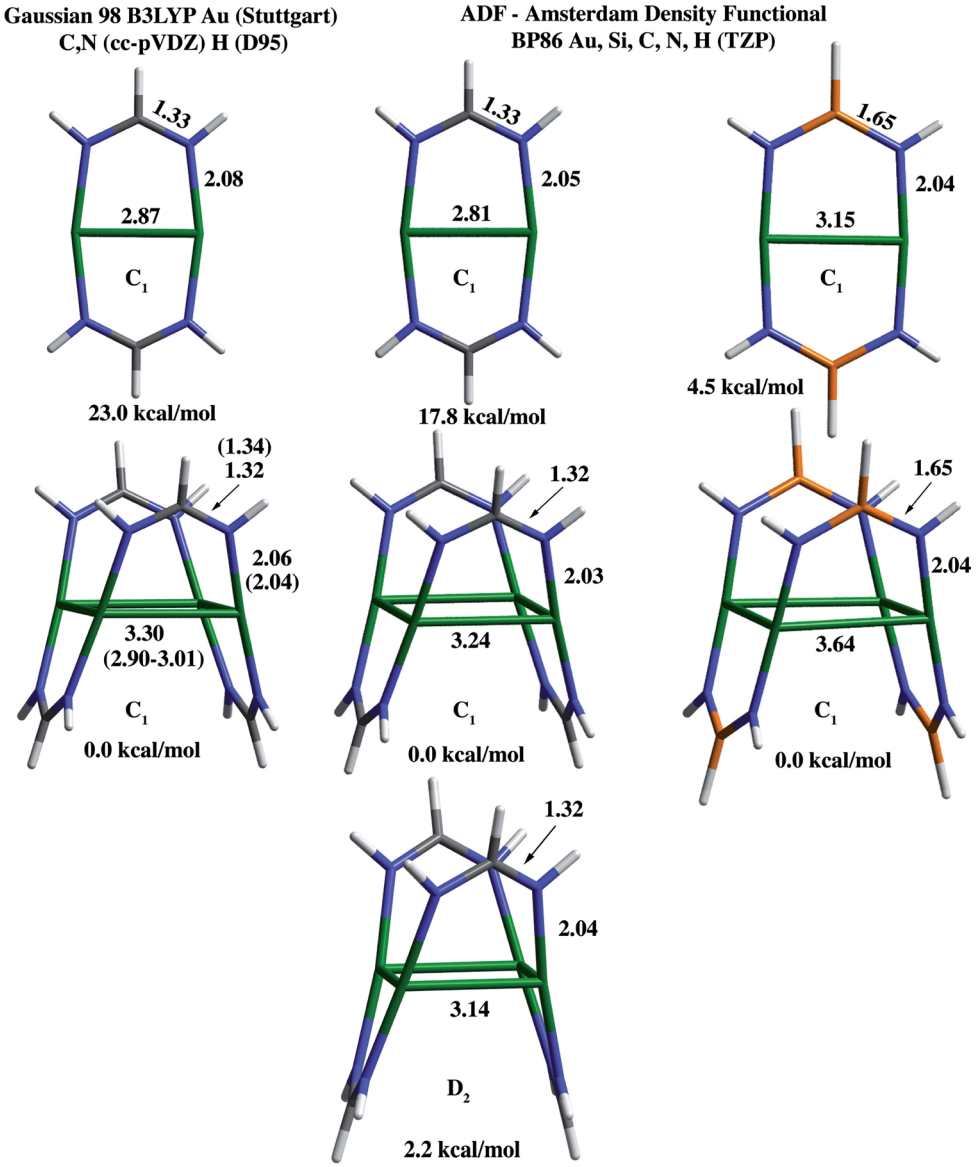

Figure 1.22 Density Functional Theory calculations of the tetranuclear and dinuclear amidinate complexes at both the Gaussian 98 and ADF levels.

isolation of the tetranuclear mixed-ligand complex $[Au_4(3,5\text{-}Ph_2pz)_3(2,6\text{-}Me_2Ph\text{-}form)]\cdot THF$. [40] These exchange reactions of the bulky amidinate ligand, $[(2,6\text{-}Me_2\text{-}form)]^-$, by the less steric ligands $[(4\text{-}MePh\text{-}form)]^-$ and $[(3,5\text{-}Ph_2pz)]^-$, are irreversible, Figure 1.23. These results validate the calculations which indicate that

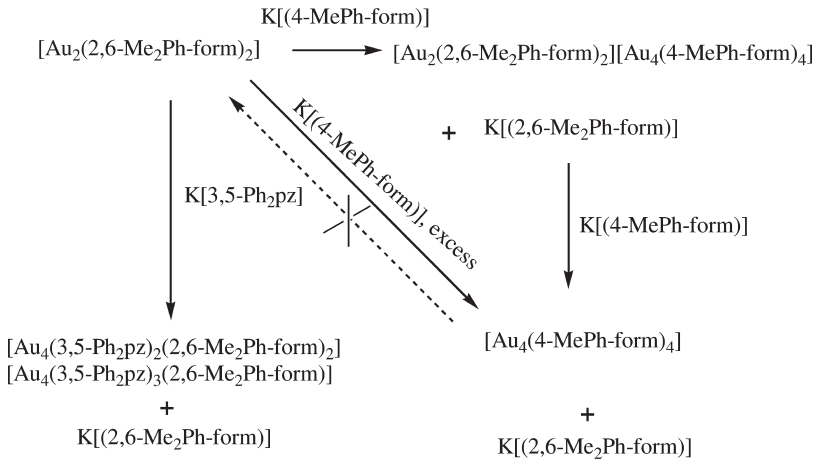

Figure 1.23 Schematic representation of the exchange reactions.

the tetranuclear structure is favored over the dinuclear arrangement with these nitrogen ligands.

The structures of the mixed ligand, dinuclear-tetranuclear Au_2Au_4 complexes show similar bond distances and angles, Au ··· Au = ∼2.7 Å, (dinuclear) and ∼3.0 Å (tetranuclear), to their parent complexes [19, 23, 34]. In the complexes [Au_4(3,5-Ph_2pz)$_2$ (2,6-Me_2-form)$_2$] and [Au_4(3,5-Ph_2pz)$_3$(2,6-Me_2-form)], the Au ··· Au dis-

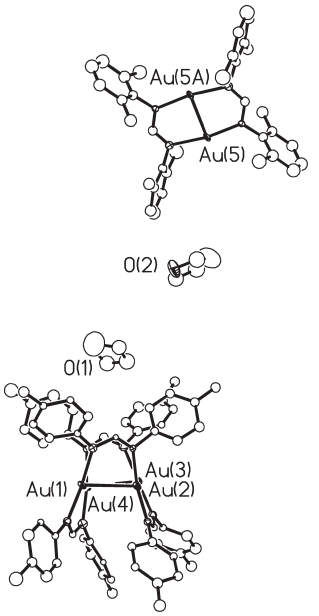

Figure 1.24 Thermal ellipsoid plot of [Au_2(2,6-Me_2Ph-form)$_2$][Au_4(4-Me-form)$_4$]·2THF.

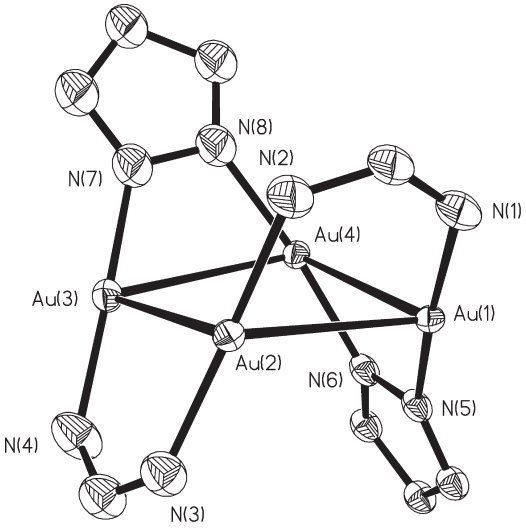

Figure 1.25 Thermal ellipsoid plot of $[Au_4(3,5\text{-}Ph_2pz)_2(2,6\text{-}Me_2\text{-}form)_2]$.

tances range from 3.02–3.20 Å. Each pyrazolate ring in $[Au_4(3,5\text{-}Ph_2pz)_2(2,6\text{-}Me_2Ph\text{-}form)_2]\cdot 2THF$ is facing an amidinate ligand, that is, *anti*. This avoids the steric bulk of the amidinate ligand, Figure 1.25. In the tetranuclear gold(I) pyrazolate complex, $[Au_4(t\text{-}Bu\text{-}pz)_4]$, the Au · · · Au distance ranges from 3.11 to 3.18 Å [16]. The Au · · · Au distances linked by the pyrazolate ligands are slightly longer than those linked by the amidinate ligands, as expected from the required orientation of the Au–N sigma bonds of the different ligands.

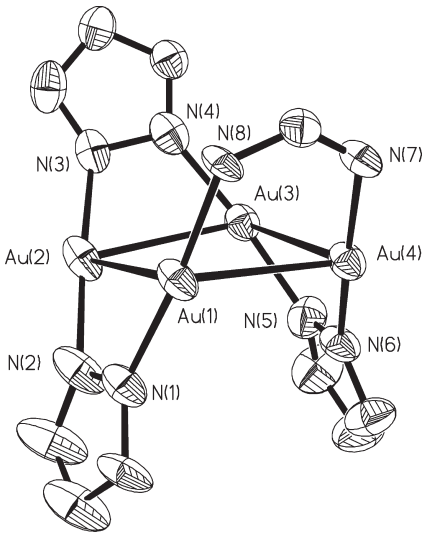

Figure 1.26 Thermal ellipsoid plot of $[Au_4(3,5\text{-}Ph_2pz)_3(2,6\text{-}Me_2\text{-}form)]$.

1.6
Solvent Influences on Oxidation and Nuclearity of Gold Guanidinate Derivatives

Work with the Hhpp ligand was pioneered by Cotton and co-workers who showed that the di-metal complexes with Cr(II), Mo(II), or W(II), ionize readily, the latter more readily than cesium [41]. Recent work with the anionic hpp ligand has produced the compound $[Au_2(hpp)_2Cl_2]$ with a short Au–Au (2.47 Å) distance [17, 18].

Although it is known that the direction of the lone pairs of electrons on nitrogen ligands can influence the nuclearity of the complexes formed, as for example, with the 3,5-diphenylpyrazolate ligand which normally forms trinuclear complexes with Au(I) or Ag(I), Figure 1.27, Raptis and coworkers [16] were able to obtain a tetranuclear Au(I) pyrazolate complex by using bulky groups at the 3 and 5 positions of the ring.

While we have been unsuccessful with many attempts by direct synthesis or reduction to isolate the gold(I) $[Au_2(hpp)_2]$, we have discovered that solvent conditions determine whether oxidation to the dinuclear Au(II) species, $[Au_2(hpp)_2Cl_2]$, occurs or a tetranuclear Au(I) species, $[Au_4(hpp)_4]$, forms. It appears that the nuclearity of the gold(I) hpp compound depends on factors such as the disproportionation rate of the Au(I) in a given solvent and the presence of oxidants. The short ligand N · · · N distance should promote tetranuclear product formation over dinuclear species but in the presence of oxidizing solvents and solvents supporting rapid disproportionation and in the presence of coordinating ligands like chloride, a gold(II) product is isolated.

This solvent role regarding the formation of a dinuclear Au(II) or a tetranuclear Au(I) product is noted when Na[hpp] is reacted with (THT)AuCl. In THF the product is the dinuclear Au(II) species, $[Au_2(hpp)_2Cl_2]$, along with gold metal. In oxidizing solvents such as the chlorocarbon dichloromethane, $[Au_2(hpp)_2Cl_2]$ is produced in high yield without Au(0) formation, Figure 1.28. If ethanol is used as the solvent, the product is the tetranuclear Au(I) species, $[Au_4(hpp)_4]$. A plausible rationalization of the different behavior in the two solvents is that ethanol solvates both the $[(THT)Au]^+$ and the Cl^-, reducing the potential of the cation for oxidation and allowing solvation of the sodium chloride. Several reducing agents were used in attempts to reduce the Au(II) complex to form the Au(I) product, including reagents such as KC_8 and K, but each produced gold metal. Using silver benzoate in a CH_3CN/THF solution to

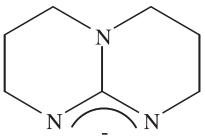

1,3,4,6,7,8-hexahydro-2H-pyramido[1,2-a]-pyramidinate

[hpp]⁻

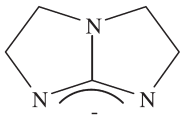

1,3,6-triazabicyclo [3.3.0]oct-4-ene

[tbo]⁻

Figure 1.27 Structure of the anionic, bidentate nitrogen ligands $[hpp]^-$ and $[tbo]^-$.

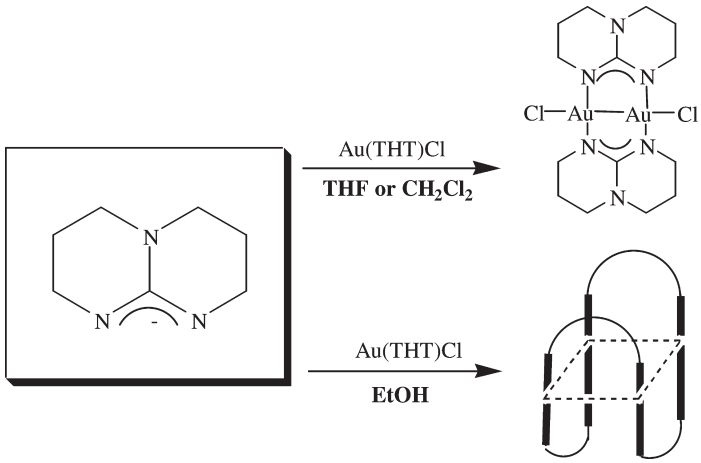

Figure 1.28 Synthesis of $[Au_2(hpp)_2Cl_2]$ and $[Au_4(hpp)_4]$.

remove the chlorides formed, a green hexanuclear product with mixed metals and ligands was achieved. The gold(II)-silver(I) complex $[(PhCOO)_6Au_4(hpp)_2Ag_2]$ crystallized and was structurally characterized. It has a very short Au–Au distance, 2.4473(19) Å, and normal Au–Ag, 3.344(3) Å, and Ag–Ag, 2.771(6) Å distances [18].

The X-ray crystal structure of $[Au_2(hpp)_2Cl_2]$ revealed a Au(II)–Au(II) distance of 2.4752(9) Å, Figure 1.29, which is shorter than the Au–Au distance observed in the amidinate, $[Au_2(2,6\text{-}Me_2Ph\text{-}form)_2Cl_2]$ (2.617 Å) [23, 24]. This decrease in distance is

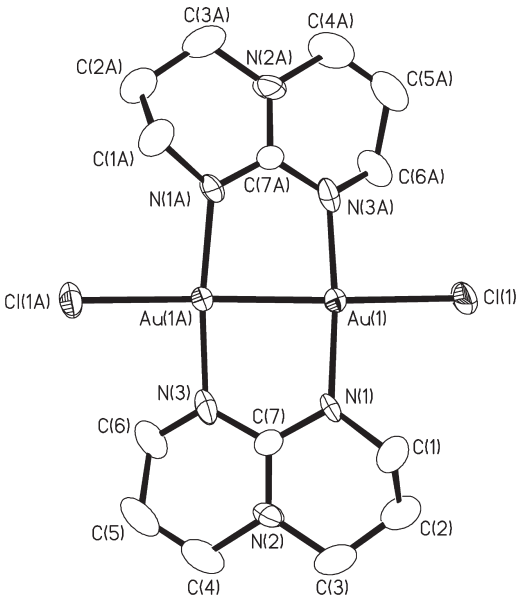

Figure 1.29 Structure of $[Au_2(hpp)_2Cl_2]$.

dramatic, and results in a stable d^9-d^9 system with the Au(II) atoms in a square planar arrangement. The coordination angles range from 86.07–94.25° and sum to 359.42°. The dihedral angle between the N(1)-Au(1)-N(3A) and N(1A)-Au(1A)-N(3) plane in $[Au_2(hpp)_2Cl_2]$ is 13.3°. The structure is puckered with deviation from the mean plane of 0.35 Å.

The molecular structures of $Mo_2(hpp)_4$ and $W_2(hpp)_4$ studied by Cotton show M–M distances of 2.067(1) and 2.162(1) Å, respectively [41]. These two complexes contain the shortest Mo_2^{4+} or W_2^{4+} quadruple bonds known. The ready oxidation of these complexes with the electron-rich bicyclic guanidinate ligand, hpp^-, and of the dinuclear gold species, clearly shows that ligands which favor short metal-metal distances promote reduction of the electron density between the metal atoms by electron loss.

The gold-gold distances in the $[Au_4(hpp)_4]$ complex, range from 2.8975(5)–2.9392 (6) Å, and are similar to those found in the tetranuclear gold amidinate complexes, Figure 1.30. The hpp ligand apparently shows a different behavior with different group 11 elements, forming a tetranuclear complex with gold and silver but to date only a dinuclear complex of copper(I) has been reported [42]. With the related smaller ring guanidinate $[Au_4(tbo)_4]$ the average Au · · · Au distance is 3.16 Å, Figure 1.31. The angles at Au · · · Au · · · Au in this complex are acute 66.03(3)–66.12(3)° and obtuse 111.92.64(3)–115.82(3)°.

Density functional theory and MP2 calculations on $[Au_2(hpp)_2Cl_2]$ show that the HOMO is predominately hpp and chlorine-based with some Au-Au δ^* character and that the LUMO has metal-to-ligand (M-L) and metal-to-metal (M-M) σ^* character (approximately 50% hpp/chlorine, and 50% gold). DFT calculations on $[Au_4(hpp)_4]$

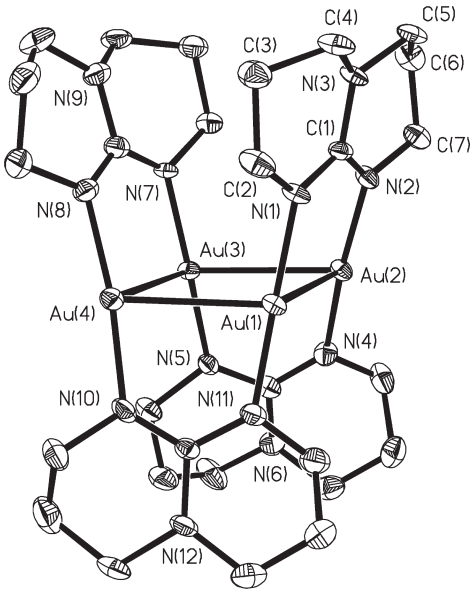

Figure 1.30 Thermal ellipsoid plot of $[Au_4(hpp)_4]$.

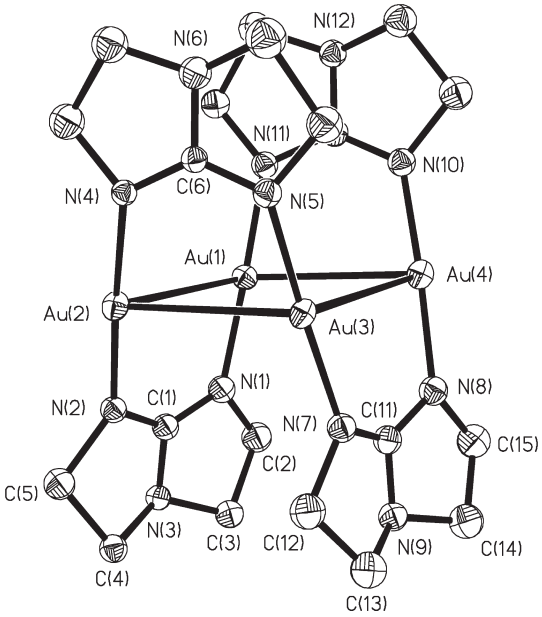

Figure 1.31 Thermal ellipsoid plot of $[Au_2(tbo)_4]$.

show that the HOMO and HOMO-1 are a mixture of metal-metal antibonding character and metal-ligand antibonding character and that the LUMO is predominately metal based s character (85% Au and 15% hpp).

The calculated thermodynamics for the reduction of $[Au_2(hpp)_2Cl_2]$ to $[Au_2(hpp)_2]$ and $Cl_2(g)$ suggest the reaction is endothermic with a ΔH° of 50.0, 48.6, 45.8, and 69.5 kcal mol^{-1} and a ΔG° of 38.3, 37.5, 35.3, and 57.8 kcal mol^{-1} depending upon the level of theory used [18]. The fact that the reaction is thermodynamically unfavorable is consistent with the difficulty in obtaining the Au(I) compound $[Au_2(hpp)_2]$.

1.7
Cyclic Trinuclear Gold(I) Nitrogen Compounds

Trinuclear 9-membered rings can be formed by the reaction of gold(I) ions with exobidentate C,N or N,N monoanionic ligands. They are generally slightly irregular and puckered unless the metallocycle is imposed by intramolecular crystallographic symmetry. Gold-gold intramolecular interactions are always present and the complexes exhibit a roughly C_{3h} or with symmetrical ligands a D_{3h} symmetry. Crystal structures of these trinuclear complexes demonstrate formation of individual complexes, dimers, supramolecular columnar species or more complex supramolecular aggregates, Table 1.4 [43]. Dimers and supramolecular structures are held together by aurophilic intermolecular gold-gold interactions. Bulky substituents on the ligands can prevent intermolecular metal-metal interactions and the formation of supramolecular architectures.

Table 1.4 Trimeric cyclic gold(I) compounds[a].

Complex	Ref
$[\mu\text{-}N^1,C^2\text{-pyAu}]_3$	[44, 45]
$[\mu\text{-}C(OMe)=N(C_6H_{11})Au]_3$	[46]
$[\mu\text{-}C(OMe)=N(Me)Au]_3$	[47, 48]
$[\mu\text{-}C(OEt)=N(C_6H_4p\text{-}Me)Au]_3$	[49, 50]
$[\mu\text{-}N^1,C^2\text{-bzimAu}]_3$	[51]
$[\mu\text{-}N,N\text{-}3,5\text{-}Ph_2pzAu]_3$	[52]
$[\mu\text{-}N,N\text{-}3,5(CF_3)pzAu]_3$	[53, 54]
$[\mu\text{-}N,N\text{-}3,5(4\text{-}MeOPh)_2pzAu]_3$	[55, 56]
$[\mu\text{-}N,N\text{-pzAu}]_3$	[57]
$[\mu\text{-}N,N\text{-}4\text{-}MepzAu]_3$	[57]

[a]py = pyridinate; bzim = 1-benzylimidazolate; pz = pyrazolate.

The first cyclic trinuclear compound of gold(I) was reported by Vaughan in 1970 [44]. The complex $[\mu\text{-}N^1,C^2\text{-pyAu}]_3$ was obtained in a very good yield by adding triphenylarsine gold(I) chloride to a THF solution of 2-pyridyllithium at −40 °C, Figure 1.32.

Some other cyclic trinuclear gold(I) pyridine complexes, CTCs, were obtained by the same procedure using various substituted pyridines [44]. All the complexes except $[\mu\text{-}N^1,C^2\text{-pyAu}]_3$ have a very low solubility in common organic solvents. In 1972, the synthesis of another CTC gold(I) complex $[\mu\text{-}C(OCH_3)=N(C_6H_{11})Au]_3$ was reported. The complex was obtained by the reaction of chloro(triphenylphosphine)gold(I) with cyclohexyl isocyanide in a methanolic potassium hydroxide solution, Figure 1.33 [46]. Using the same or similar synthetic approaches, many other analogous carbeniate cyclic gold(I) complexes have been described [47, 49]. They have the general formula $[\mu\text{-C,N-carbAu}]_3$ (carb is C(OR)=NR′) where R′ is an aliphatic, alicyclic, alkyl aromatic or aromatic group, Figure 1.33.

Another family of gold(I) CTCs, having a C-Au-N environment, was described in which the bridging ligand between gold atoms is an alkyl-2-imidazolate anion (alkyl group = CH_3 or CH_2Ph) [51]. A typical reaction is carried out at −40 °C in THF using Vaughan's method, Figure 1.34, but in this case the crude brown solid is extracted

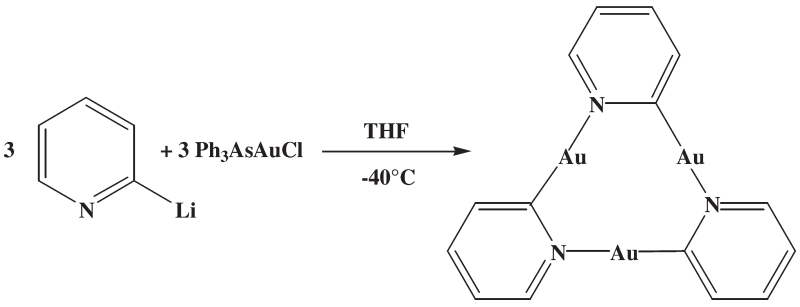

Figure 1.32 Synthesis of $[\mu\text{-}N^1,C^2\text{-pyAu}]_3$.

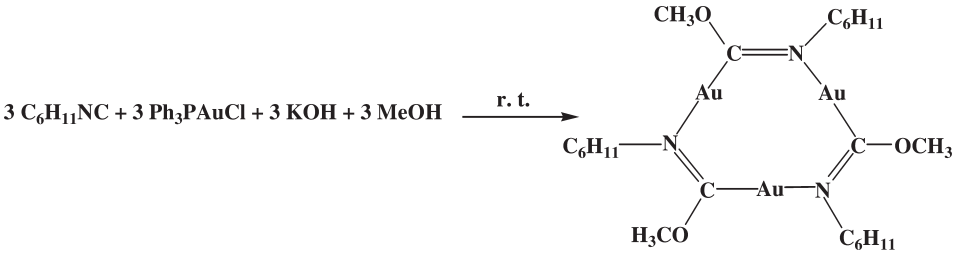

Figure 1.33 Synthesis of [μ-C(OCH$_3$)=N(C$_6$H$_{11}$)Au]$_3$.

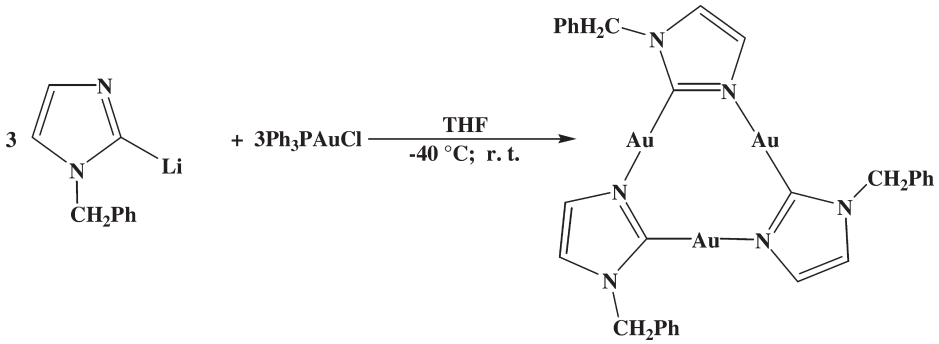

Figure 1.34 Synthesis of [μ-N^1,C^2-bzimAu]$_3$.

overnight at room temperature with hexane. The reaction can be carried out using $(CH_3)_2SAuCl$ as a starting material instead of Ph_3PAuCl. In this way the CTCs [μ-C(OEt)=N(C$_6$H$_4$-*p*-Me)Au]$_3$ and [μ-N^1,C^2-bzimAu]$_3$ are immediately formed in a good yield, but the reaction is delicate and slow and often colloidal gold(0) is formed. The methyl analog of [μ-N^1,C^2-bzimAu]$_3$ is quite soluble in the common organic solvents.

Gold(I) CTCs having a N-Au-N environment are also known and have the general formula [μ-N,N-pzAu]$_3$ (pz$^-$ = pyrazolate or various ring substituted pyrazolates) [15b,52,53,55]. In these compounds the bidentate anion ligands bridging the gold atoms are obtained by deprotonation of a pyrazole ring with a base such as KOH or NaH, Figure 1.35 [15b]. It is noteworthy that when Na[3,5-Ph$_2$pz] and AgO_2CPh are added to a THF solution of Ph_3PAuCl a hexanuclear gold cycle having a 18-atom ring is formed [15b].

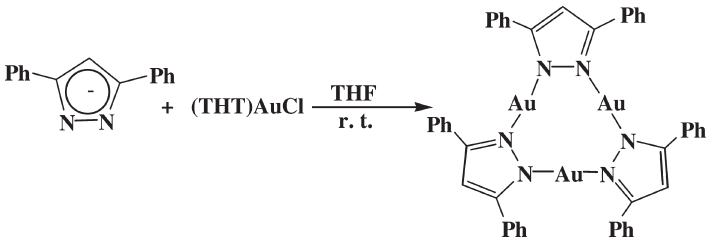

Figure 1.35 Synthesis of [μ-N,N-3,5-Ph$_2$pzAu]$_3$.

The cyclic trimeric nature of the carbeniate Au(I) complexes was realized when the structure of [μ-C(OEt)=N(C_6H_4-*p*-Me)Au]$_3$ was reported [50]. This structure is a 9-membered ring formed by three carbeniate ligands bridging the gold(I) atoms through the N and C atoms. The deviation of the C-Au-N angles from the linearity as well as the puckering of the rings are due to the presence of intramolecular (average Au $\cdots$ Au = 3.272(1) Å) and intermolecular gold-gold interactions. Only two short Au $\cdots$ Au contacts of 3.244(1) Å are found between two CTCs, and the dimer is arranged in the crystal structure to give a characteristic Au_6 chair. The packing diagram of [μ-C(OEt)=N(C_6H_4-*p*-Me)Au]$_3$ shows additional weak Au(I) $\cdots$ Au(I) interactions at 3.824 Å.

The Au–Au distance in [μ-C(OMe)=N(Me)Au]$_3$ of 3.308(2) Å suggests an intramolecular interaction between the metal atoms [48]. The most important and unique feature of the complex [μ-C(OEt)=N(C_6H_4-*p*-Me)Au]$_3$ is the ability of the CTCs to aggregate in the solid state along the *c* axis to form ordered and disordered columnar stacks. In each unit cell, the two types of stacks occur in a 2 : 1 ratio. In the ordered stacks the intermolecular Au $\cdots$ Au distance is 3.346(1) Å and the gold centers are arranged to form an infinite trigonal prismatic array. In the disordered stacks there are two sets of positions for each gold triangle. The ability of the complex [μ-C(OEt)=N(C_6H_4-*p*-Me)Au]$_3$ to aggregate through gold-gold intermolecular interactions forming these supramolecular arrays confers to its extraordinary luminescent properties which have been described by Balch as solvoluminescence [48].

The complex [μ-N^1,C^2-pyAu]$_3$ shows an interesting and unusual crystal structure. It is located on a crystallographic mirror plane that lies perpendicular to the molecular plane. Each CTC is planar with gold-gold intramolecular interactions of 3.309(2) and 3.346(3) Å. The intermolecular Au $\cdots$ Au contacts are shorter than the intramolecular Au $\cdots$ Au contacts and fall in the range 3.105(2)-3.143(3) Å. Both CTC complexes [μ-N^1,C^2-pyAu]$_3$ and [μ-C(OMe)=N(C_6H_{11})Au]$_3$ form dimers with a chair conformation of the gold atoms, but complex [μ-N^1,C^2-pyAu]$_3$ is further assembled by the apical gold atoms of the chairs to form extended stepwise chains.

Recently, gold pyrazolate CTCs have been described which produce room-temperature columnar mesophases [55]. These complexes have long chain substituents in the 3 and 5 positions of the pyrazolate ring. X-ray powder diffraction measurements have demonstrated that the supramolecular columnar arrangement is present in the crystalline solids as well as in the mesomorphic phase. The X-ray crystal structure of complex [μ- N,N-3,5(4′-MeOPh)$_2$pzAu]$_3$ which has an anisole unit on the pyrazolates, yields a unit cell which contains two independent CTCs. They are slightly different in the twist about the central metallocycle core and more markedly in the relative conformations of the phenyl substituents [56]. In the complex [μ-N,N-3,5(4′-MeOPh)$_2$pzAu]$_3$ the intramolecular Au $\cdots$ Au average distance is 3.3380(7) Å. The intermolecular Au $\cdots$ Au distance is greater than 4.252 Å with a mean stacking separation between two consecutive trimers of 4.54 Å. The packing mode observed appears to be controlled by van der Waals forces (i.e., no Au $\cdots$ Au interactions).

A more complex supramolecular architecture has been discovered for the complexes [μ-N,N-pzAu]$_3$, Figure 1.36, and [μ-N,N-4-MepzAu]$_3$ [57]. Intramolecular

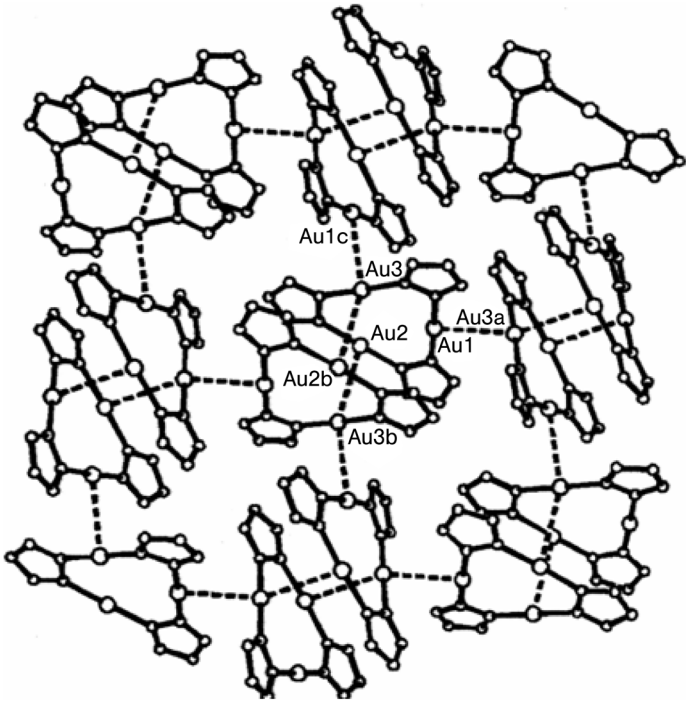

Figure 1.36 Two dimensional structure of $[\mu\text{-N,N-pzAu}]_3$.

aurophilic gold-gold interactions are present with Au · · · Au distances of 3.372(1)-3.401(1) Å. Complex $[\mu\text{-N,N-pzAu}]_3$ forms a two-dimensional network by self-assembly of the CTCs through intermolecular aurophilic interactions. Each $[\mu\text{-N,N-pzAu}]_3$ forms a dimer such as those found in other CTCs, with two gold-gold interactions of 3.313(1) Å. Moreover, each dimer interacts with four other dimers through a single Au · · · Au contact 3.160(1) Å to form a 2-dimensional net.

1.8
Oxidative-Addition Reactions to the Cyclic Trinuclear Gold(I)-Nitrogen Compounds

Gold CTCs undergo oxidative-addition reactions of halogens at the metal centers [58]. There is evidence that electronic factors influence the reactivity of the gold atoms in these compounds. In fact, except for $[\mu\text{-C(OMe)=N(Me)Au}]_3$, only one metal center appears to be oxidized to give mixed-valence Au_2^I/Au^{III} metallocycles. Surprisingly, aqua regia also fails to give complexes beyond the Au_2^I/Au^{III} oxidation state with the unoxidized pyrazolates. Thus an unusual stability of the $d^{10}d^{10}d^8$ configuration for these pyrazolate gold CTCs is observed. The electronic communication between the gold atoms may be the origin of this effect. The oxidation of the first gold atom may improve the π-acceptor ability of the two ligands coordinated to it so that they remove sufficient electron density from the remaining two Au^I atoms and prevent

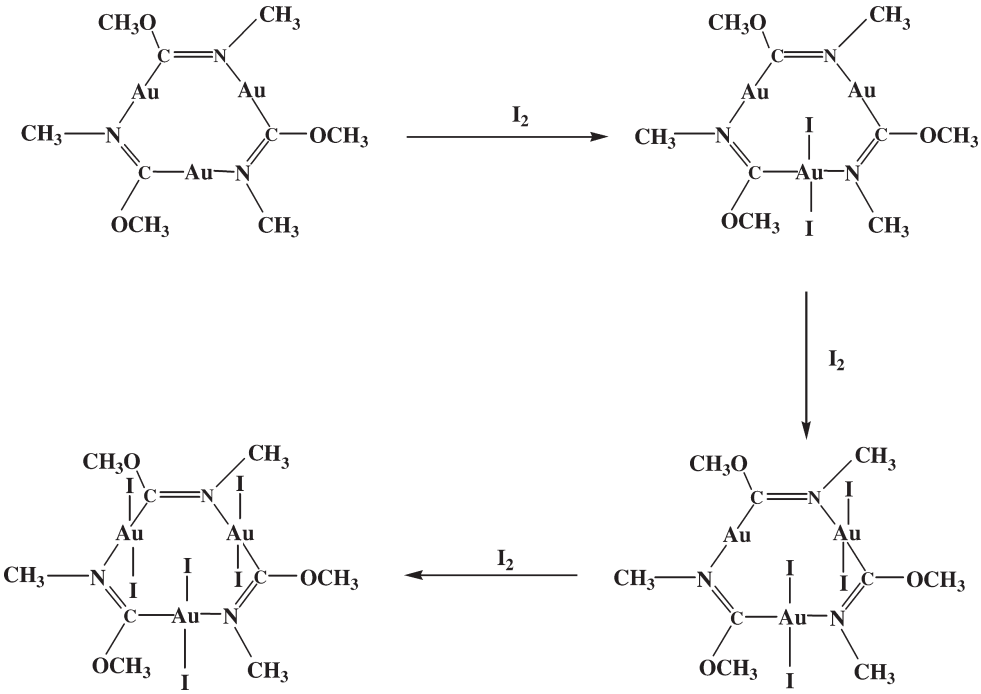

Figure 1.37 Synthesis of the mixed-valence or completely oxidized complexes $[\mu\text{-C(OMe)=N(Me)Au}]_3I_n$ ($n = 2$–6).

their oxidation. However this hypothesis is not corroborated by the crystallographic data since change is not observed in the gold-ligand bond lengths. However the effect may involve Au-N pi interactions with subsequently little atom movement. The complex $[\mu\text{-C(OMe)=N(Me)Au}]_3$ seems to be unique in the family of the gold CTCs and to date it is the only CTC of gold(I) that gives the stepwise addition of halogens, resulting in the formation of either mixed-valent or completely oxidized trinuclear gold complexes, Figure 1.37. The X-ray structures of these derivatives were recently reported many years later after their synthesis [58].

Crystallographic studies of the iodine oxidized carbeniate $[\mu\text{-C(OMe)=N(Me)Au}]_3$ confirms the structures originally proposed [58]. All the structures retain the frame of the starting complex $[\mu\text{-C(OMe)=N(Me)Au}]_3$, Figure 1.38. The variation in the intramolecular Au $\cdots$ Au separation is small. However, there is a trend toward increased Au $\cdots$ Au distance as more iodine is added to the complex. The Au–I distances fall in the range of 2.614(6)-2.633(7) Å. As a consequence of the repulsive intramolecular I $\cdots$ I contacts, the I-Au-I angles deviate significantly from linearity. They become smaller and smaller with increased number of iodide atoms bonded to the gold centers. The structure of $[\mu\text{-C(OMe)=N(Me)Au}]_3I_6.CH_2Cl_2$ shows the formation of columns with short intermolecular I $\cdots$ I interactions ranging from 3.636(2) to 3.716(2) Å. The interaction between terminal iodide ligands appears to have a directional component.

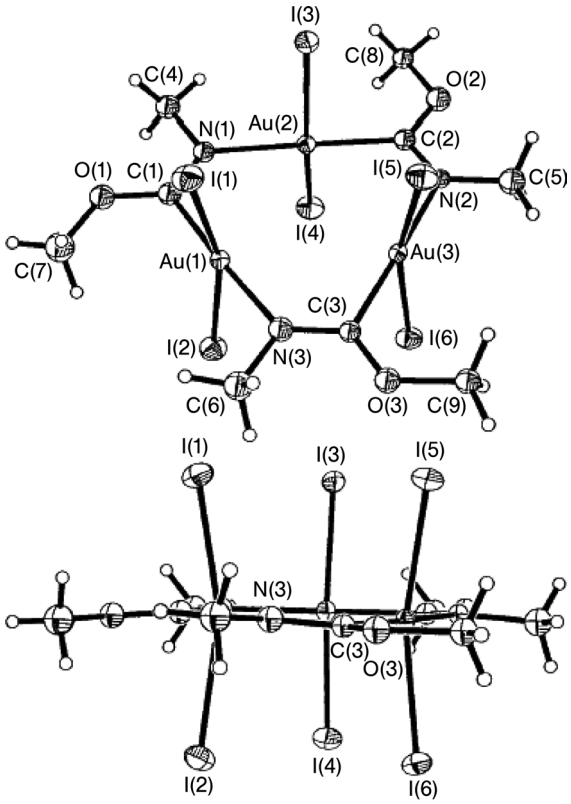

Figure 1.38 Top and side views of the completely oxidized complex [μ-C(OMe)=N(Me)Au]$_3$I$_6$.

Oxidative-addition of iodine also was investigated for the complex [μ-N^1, C^2-bzimAu]$_3$. This complex behaves like most of the CTCs since it adds iodine at only one gold center to yield [μ-N^1,C^2-bzimAu]$_3$I$_2$ [59]. The X-ray structure shows that it consists of discrete trinuclear units with the three gold atoms bridged by 1-benzylimidazolates.

1.9
Supramolecular Entities of Trinuclear Gold(I) Complexes Sandwiching Small Organic Acids

Extended linear chain inorganic compounds have special chemical and physical properties [60, 61]. This has led to new developments in fields such as supramolecular chemistry, acid-base chemistry, luminescent materials, and various optoelectronic applications. Among recent examples are the developments of a vapochromic light emitting diode from linear chain Pt(II)/Pd(II) complexes [62], a luminescent switch consisting of an Au(I) dithiocarbamate complex that possesses a luminescent linear

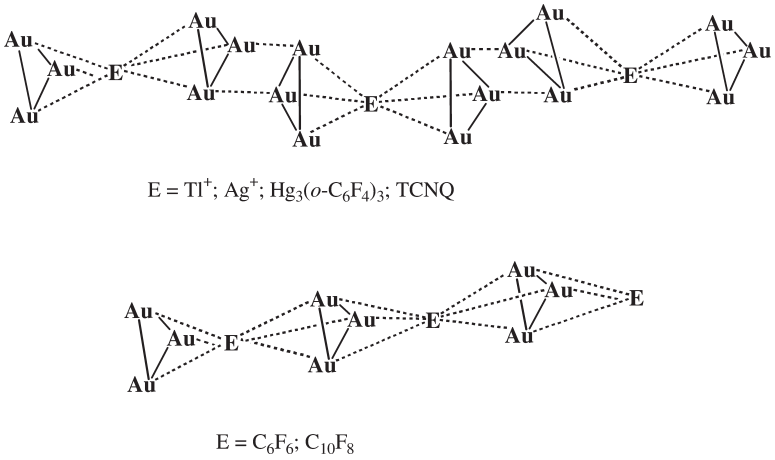

Figure 1.39 Structural arrangements of the cyclic trinuclear Au^{I} compounds, CTCs, with various electrophilic adducts in ABBA and ABA chains.

chain in the presence of vapors of organic solvents [31], mixed-metal (Ag/Au or Tl/Au) [63] compounds that exhibit different colors and emissions when different organic solvents are introduced or removed, and the discovery of solvoluminescence [48] in a Au(I) CTC with an extended chain structure.

Recent results have demonstrated that the electron-rich trinuclear Au(I) complexes can interact with neutral electron-acceptor entities such as C_6F_6, $C_{10}F_{14}$, TCNQ, or $Hg_3(\mu\text{-}C_6F_4)_3$, and cation species such as Ag(I) and Tl(I) to produce infinite linear chain complexes, Figure 1.39 [64–66]. Balch and co-workers also demonstrated that trinuclear Au(I) compounds with alkyl-substituted carbeniate bridging ligands can interact with the large organic acceptors nitro-9-fluorenones [67]. DFT calculations clearly show that the donor regions in the trinuclear Au(I) compounds are located at the center of the 9-membered ring and that they extend to regions in space above and below the ring plane [63].

The TCNQ molecule in $[TR(bzim)]_2{\cdot}TCNQ$ is sandwiched between two units of $[\mu\text{-}N^1,C^2\text{-}bzimAu]_3$ in a face-to-face manner so that it is best represented by the formula $(\pi\text{-}[\mu\text{-}N^1,C^2\text{-}bzimAu]_3)(\mu\text{-}TCNQ)(\pi\text{-}[\mu\text{-}N^1,C^2\text{-}bzimAu]_3)$. The cyanide groups clearly are not coordinated to the gold atoms. The distance between the centroid of TCNQ to the centroid of the Au_3 unit is 3.964 Å. The packing of $[TR(bzim)]_2{\cdot}TCNQ$ shows a stacked linear-chain structure with a repeat pattern of $\text{-}(Au_3)(Au_3)(\mu\text{-}TCNQ)(Au_3)(Au_3)(\mu\text{-}TCNQ)\text{-}$ an ABBABB repeat. The complex $[TR(bzim)]_2{\cdot}TCNQ$ contains two very short intermolecular Au $\cdots$ Au distances of 3.152 Å (identical for the two aurophilic bonds). The intermolecular Au $\cdots$ Au distance is even shorter than the intramolecular distances in the starting compound, which are 3.475, 3.471, and 3.534 Å. The adjacent Au_3 units in $[TR(bzim)]_2{\cdot}TCNQ$ form a chair-type structure rather than the face-to-face (nearly eclipsed) pattern reported in Balch's studies of the nitro-9-fluorenones adducts with the trinuclear Au(I) alkyl-substituted carbeniate complexes.

The shortened intermolecular Au–Au distances in $[TR(bzim)]_2 \cdot TCNQ$ may be associated with charge-transfer from the electron-rich Au center to the known electron acceptor TCNQ. A partial oxidation of the Au(I) atoms leads to the observed shortening of Au–Au distances. In the limit of complete oxidation to Au(II), a gold-gold single bond forms with $[TCNQ]^-$. The presence of $[TCNQ]^-$ impurity in the crystals may be the origin of the dark color of this complex since $[TR(bzim)]_2$ itself is colorless while TCNQ is light orange. Thin crystals and films are dark green as are solutions. It remains possible that charge transfer is the cause of the dark color, with adduct formation remaining intact in solution.

The crystal structure of $[TR(carb)] \cdot C_6F_6$ shows a columnar stack consisting of alternating C_6F_6 and [TR(carb)] molecules [65]. The C_6F_6 molecule is sandwiched between two units of [TR(carb)], in a face-to-face manner so that a molecule of $[TR(carb)] \cdot C_6F_6$ is best represented by the formula $(\pi\text{-}[TR(carb)])_{0.5}(\mu\text{-}C_6F_6)(\pi\text{-}[TR(carb)])_{0.5}$. The distance between the centroid of C_6F_6 to the centroid of the Au_3 unit is 3.565 Å. The packing of $[TR(carb)] \cdot C_6F_6$ shows a stacked linear-chain structure with a repeat pattern of $\cdot(Au_3)(\mu\text{-}C_6F_6)(Au_3)(\mu\text{-}C_6F_6)\cdot$ an ABAB pattern. The crystal structure of [TR(carb)] by itself shows a dimeric structure with intermolecular Au-Au bonds. Therefore, the C_6F_6 Lewis acid disrupts the intermolecular aurophilic bonding in [TR(carb)] chain with loss of visible luminescence [65]. These pi-acid, pi-base results with gold CTCs are similar to but opposite from the interactions reported by Gabbaï and co-workers, between the Lewis acid $Hg_3(\mu\text{-}C_6F_4)_3$ and benzene, in which benzene acts as a Lewis base coordinating in a μ-6 manner to six Hg centers, three from each side [68, 69]. The two Au_3 units interacting with C_6F_6 in $[TR(carb)] \cdot C_6F_6$ are eclipsed with respect to each other (nearly D_{3h}) whereas the two Hg_3 units in $Hg_3(\mu\text{-}C_6F_4)_3 \cdot$benzene are nearly staggered (D_{3d}).

The Lewis acid $Hg_3(\mu\text{-}C_6F_4)_3$ also forms a pi-acid/pi-base interaction with TR(carb). In addition to the crystal structure demonstrating the ABBABB pattern observed in other stacked materials which retain the aurophilic Au–Au interactions between four of the six basic Au(I) atoms of the BB moieties, studies have shown that the oligomeric acid/base interection is retained in solution. Pulsed gradient diffusion NMR studies [70] suggesting the oligomeric sizes and ^{13}C-^{19}F coupling between units demonstrate that the interactions are stronger than solvation of the CDCs.

The nucleophilic trinuclear Au(I) ring complex $Au_3(p\text{-tolN=COEt})_3$, Figure 1.40, forms sandwich adducts with the organic Lewis acid octafluoronaphthalene, $C_{10}F_8$ [66]. The $Au_3(p\text{-tolN=COEt})_3 \cdot C_{10}F_8$ adduct has a supramolecular structure consisting of columnar interleaved 1 : 1 stacks in which the $Au_3(p\text{-tolN=COEt})_3$ π-base molecules alternate with the octafluoronaphthalene π-acid molecules with a distance between the centroid of octafluoronaphthalene to the centroid of $Au_3(p\text{-tolN = COEt})_3$ of 3.458 and 3.509 Å. The stacking with octafluoronaphthalene completely quenches the blue photoluminescence of $Au_3(p\text{-tolN=COEt})_3$, which is related to inter-ring Au–Au bonding, and leads to the appearance of a bright yellow emission band observed at room temperature. The structured profile, the energy, and the lifetime indicate that the yellow emission of the $Au_3(p\text{-tolN=COEt})_3 \cdot C_{10}F_8$ adduct is due to gold influenced phosphorescence of the octafluoronaphthalene.

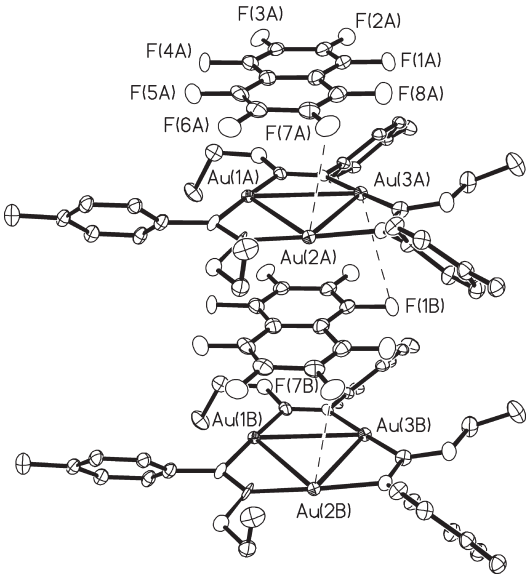

Figure 1.40 Thermal ellipsoid drawing of the stacked octafluoronaphthalene with Au_3(*p*-tolN = COEt)$_3$.

The 3.5 ms lifetime of the yellow emission of Au_3(*p*-tolN=COEt)$_3 \cdot C_{10}F_8$ is two orders of magnitude shorter than the lifetime of the octafluoronaphthalene phosphorescence which is observed at low temperature, thus indicating a gold heavy-atom effect.

1.10
Gold(I) and Silver(I) Mixed-Metal Trinuclear Complexes

Attention has been given to the synthesis of bimetallic silver-gold clusters [71] due to their effective catalytic properties, resistance to poisoning, and selectivity [72]. Recently molecular materials with gold and silver nanoclusters and nanowires have been synthesized. These materials are considered to be good candidates for electronic nanodevices and biosensors [73].

Based on the fact that pi-acids interact with the trinuclear gold(I) pi-bases, TR(carb) and TR(bzim), the trinuclear 3,5-diphenylpyrazolate silver(I) complex was reacted with each. Mixing [Au_3(carb)$_3$] or [Au_3(bzim)$_3$] with [Ag_3(μ-3,5-Ph_2pz)$_3$] in CH_2Cl_2 in stoichiometric ratios of 1 : 2 and 2 : 1 produced the mixed metal/mixed ligand complexes in the same gold-silver ratios. The crystalline products were not the expected acid-base adducts. It is suspected that the lability of the M–N bond (M=Au, Ag) in these complexes results in the subsequent cleavage of the cyclic complexes to produce the products statistically expected from the stoichiometry of materials used [74]. As a result of the lability of Au–N and Ag–N bonds, and the stability of

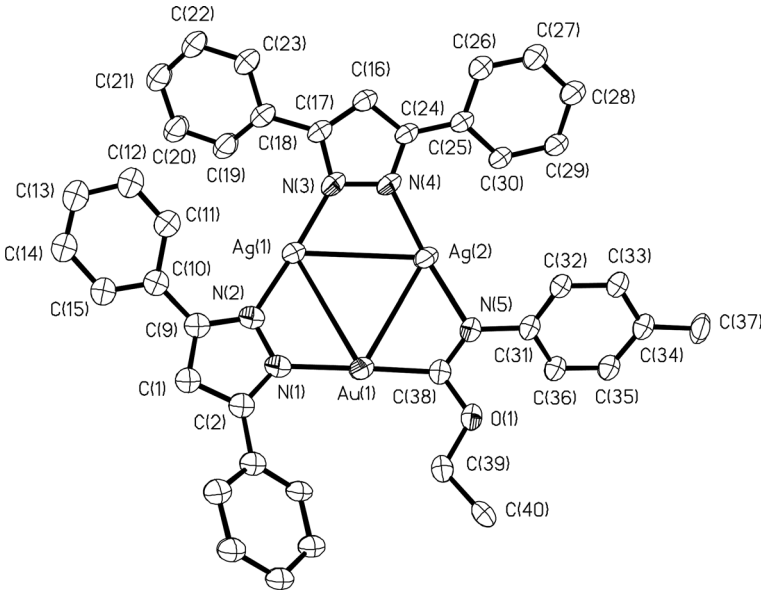

Figure 1.41 ORTEP diagram of $[Au(carb)Ag_2(\mu\text{-}3,5\text{-}Ph_2pz)_2]$.

Au–C bonds, mixed metal gold-silver dimers of planar, trinuclear complexes are readily formed by mixing gold(I) carbeniates and gold(I) benzylimidazolates with silver(I) pyrazolates in stoichiometric ratios. The complexes retain the ligands associated with the metal atoms of the starting materials.

The two trinuclear moieties of the dimer of $[Ag_3(\mu\text{-}3,5\text{-}Ph_2pz)_3]$ are rotated *anti* to each other [75], but this arrangement is less apparent in $[Au(carb)Ag_2(\mu\text{-}3,5\text{-}Ph_2pz)_2]$, Figure 1.41. The shortest Ag · · · Ag interactions within the metallocycle rings of the dimer of $[Ag_3(\mu\text{-}3,5\text{-}Ph_2pz)_3]$ are about 3.4 Å, while between the trinuclear units the Ag · · · Ag distance is 2.9712(14) Å. The Au · · · Ag distances between trinuclear units in $[Au(carb)Ag_2(\mu\text{-}3,5\text{-}Ph_2pz)_2]$ are 3.311(2) Å and 3.082(2) Å. The metallocycles in $[Au(carb)Ag_2(\mu\text{-}3,5\text{-}Ph_2pz)_2]$ are irregular and puckered similar to those in the dimer of $[Ag_3(\mu\text{-}3,5\text{-}Ph_2pz)_3]$. The structure of $[Au_2(carb)_2Ag(\mu\text{-}3,5\text{-}Ph_2pz)]$, Figures 1.42 and 1.43, shows one intermolecular interaction between the trinuclear gold units, with a Au · · · Au distance of 3.33 Å. This is slightly longer than Au · · · Au distances, 3.224–3.299 Å, in the irregular and puckered nine-membered ring of the dimer of $[Au_3(carb)_3]$. The Au · · · Ag distances in $[Au_2(carb)_2Ag(\mu\text{-}3,5\text{-}Ph_2pz)]$ are 3.22–3.28 Å. The average distance of the two closest Au atoms between the trinuclear units of each dimer is 3.2 Å. A packing diagram shows a Au · · · Au interaction, 3.857 Å, between the dimer units, similar to the distance observed in $[Au_3(carb)_3]$, 3.824 Å. The inter-trinuclear Au · · · Ag interactions in $[Au(bzim)Ag_2(\mu\text{-}3,5\text{-}Ph_2pz)_2]$ is 3.1423(8). The intermolecular distances, Au · · · Ag, 3.53 and 3.38 Å and Ag · · · Ag 3.35 Å are longer than those in the dimer of $[Au(carb)Ag_2(\mu\text{-}3,5\text{-}Ph_2pz)_2]$.

A few additional structural comparisons between the homonuclear gold and silver complexes and the mixed gold and silver complexes are of interest. In the dimer of the

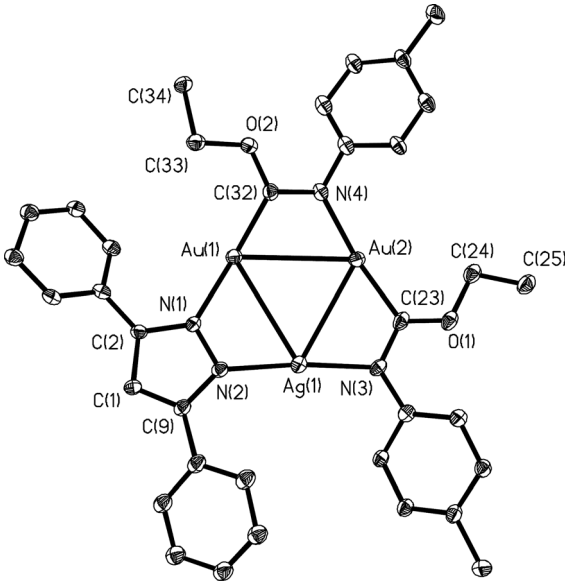

Figure 1.42 ORTEP diagram of $[Au_2(carb)_2Ag(\mu\text{-}3,5\text{-}Ph_2pz)]$.

trinuclear silver(I) 3,5-diphenylpyrazolate, $[Ag_3(\mu\text{-}3,5\text{-}Ph_2pz)_3]$, the six silver atoms are arranged as two triangles connected by only one short interaction. This drastically changes when a gold atom is introduced into the trinuclear unit as in $[Au(carb)Ag_2(\mu\text{-}3,5\text{-}Ph_2pz)_2]$. An irregular square is formed by two Ag and two Au atoms with M-M distances in the range 3.08–3.40 Å. The other two silver atoms are above and below the plane of the square. A metallophilicity is observed in $[Au(carb)Ag_2(\mu\text{-}3,5\text{-}Ph_2pz)_2]$ in which each of the two gold atoms interact with three silver atoms. Three

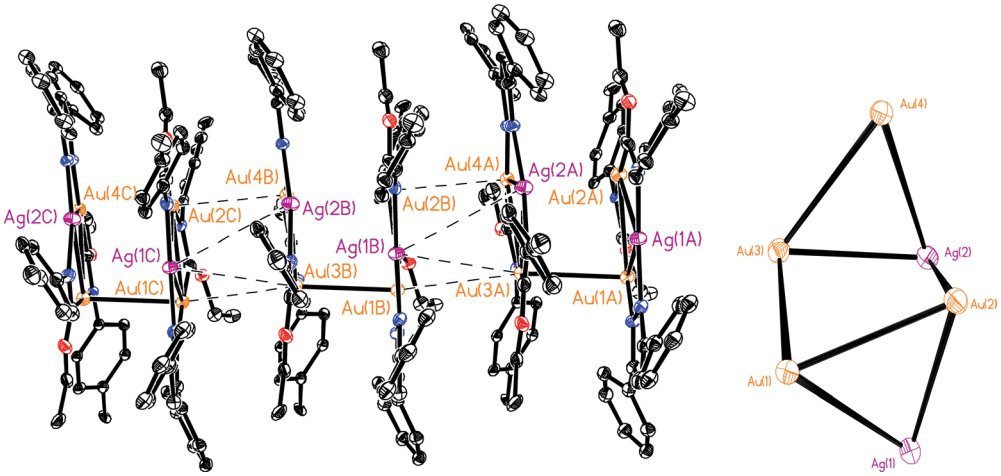

Figure 1.43 Packing diagram of$[Au_2(carb)_2Ag(\mu\text{-}3,5\text{-}Ph_2pz)]_2$.

Au atoms and one Ag atom form a nearly regular square with distances range 3.21–3.42 Å.

Ligand bridged metal-metal distances display longer M–M distances than in the unbridged complexes. In the compounds studied, the non-bridged intermolecular M-M distances follow the order: Ag–Ag < Au–Ag < Au–Au while the intra-metallocycle M–M distances with bridging ligand bonding follow the order: Au–Au < Au–Ag < Ag–Ag. The synthesis of these mixed gold-silver compounds represents a new approach to cluster mixed metal synthesis with potential use in mixed-metal catalysis.

1.11 CO Oxidation Over Au/TiO_2 Prepared from Gold Nitrogen Complexes

Metal-organic and organometallic complexes have been widely used in the synthesis of catalysts, however, the use of metal-organic or organometallic gold complexes as catalyst precursors has been limited [76]. Gates and coworkers have reported that a supported mononuclear gold complex is active for ethylene hydrogenation at 353 K [77].

A series of Au/TiO_2 catalysts have been prepared from precursors of various metal-organic gold complexes (Au_n, $n = 2$–4) and their catalytic activity for CO oxidation studied. The Au/TiO_2 catalyst synthesized from a tetranuclear gold complex shows the best performance for CO oxidation with the TEM image of this catalyst indicating an average gold particle size of 3.1 nm.

Several factors may contribute to the high activity of our Au/TiO_2 catalysts. First, the use of metal-organic complexes as precursors can avoid the use of chloride. $HAuCl_4$ is widely used as a gold precursor in catalytic studies, invariably leaving a chloride residue in the catalyst after preparation. Recently, both experimental and theoretical studies have shown that chloride can poison the catalytic performance of gold catalysts for CO oxidation. Oh *et al.* have shown that chloride residue on a catalyst can promote agglomeration of Au particles during heat treatment, and can inhibit the catalytic activity by poisoning the active site [78]. Density functional calculations show that chloride can act as a poison by weakening the adsorption of O_2 and lowering the stability of the $CO{\cdot}O_2$ intermediate complex [79]. Clearly metal-organic precursors provide an attractive route for the preparation of chloride-free gold catalysts. Another explanation for the high activity of our Au/TiO_2 catalysts also relates to the use of metal-organic precursor complexes. Upon deposition onto the oxide support, these complexes interact with the surface OH groups and become less mobile compared with gold atoms deposited using $HAuCl_4$. The catalyst particles appear to form at defect sites on the oxide as established by studies with MgO as the oxide surface. The defect sites may serve as calcination sites for the metal-organic catalyst precursors and perhaps inhibit agglomeration of gold particles during calcination. Factors preventing the sintering of gold lead to a narrow particle size distribution compared to the deposition-precipitation method of catalyst formation.

1.12 Miscellaneous Observations

The nearly simultaneous observation by the Schmidbaur [80] and Fackler [81] groups of the easy transmetallation of gold(I) with tetraphenylborate, which can be done in water, has caused Gray to develop this chemistry [82] in a general way with boronic acids. The considerable interest in the use of gold compounds as homogeneous catalysts [83] has prompted these studies. Recently Gray has described boronic acid transammination procedures to synthesize 3-coordinate azadipyrromethene complexes of gold(I) in order to examine their low energy absorption and emission properties. While the emission in the reported Au–N compound is comparable to what had been observed with the free azadipyrromethene ligand, the quantum yield is much lower. However, as Gray states [84], "The controlled auration of aromatic molecules affords access to broad classes of triplet-state luminophores and provides opportunities in materials design and organometallic photochemistry."

Acknowledgement

The Robert A. Welch Foundation of Houston, Texas is acknowledged for financial support of this work.

References

1 Fackler, J.P. (2002) Forty-five years of chemical discovery including a golden quarter-century. *Inorganic Chemistry*, **41**, 6959–6972.

2 (a) Schmidbaur, H. (ed.) (1999) *Gold Progress in Chemistry, Biochemistry, and Technology*, John Wiley & Sons, Ltd, Chichester, UK; (b) Grohman, A. and Schmidbaur, H. (1995) *Comprehensive Organometallic Chemistry II*, Vol. 3, (eds E.W. Abel, F.G. Stone and G. Wilkinson), Pergamon, Oxford, UK, pp. 1–56.

3 Puddephatt, R. (1978) *The Chemistry of Gold*, Elsevier, Oxford, UK.

4 Cotton, F.A. (1995) *Basic Inorganic Chemistry*, Vol. 3, John Wiley & Sons, New York.

5 Gimeno, M.C. and Laguna, A. (2004) *Comprehensive Coordination Chemistry II*, Vol. 6, Silver and Gold (eds J.A. McCleverty, T.J. Meyer and D.E. Fenton), Elsevier Pergamon, Oxford, UK.

6 (a) Clerac, R., Cotton, F.A., Dunbar, R.A., Murillo, C.A. and Wang, X. (2001) Dinuclear and Heteropolynuclear Complexes Containing Mo_2^{4+} Units. *Inorganic Chemistry*, **40**, 420–426; (b) Cotton, F.A., Lin, C. and Murillo, C.A. (2000) A Reliable Method of Preparation for Diiridium Paddlewheel Complexes: Structures of the First Compounds with Ir_2^{5+} Cores. *Inorganic Chemistry*, **39**, 4574–4578; (c) Cotton, F.A., Daniels, L.M., Murillo, C.A. and Schooler, P. (2000) Chromium(II) complexes bearing 2-substituted N,N′-di(aryl)formamidinate ligands. *Journal of the Chemical Society, Dalton Transactions*, (13), 2007–2012; (d) Cotton, F.A., Daniels, L.M., Murillo, C.A. and Schooler, P. (2000) Chromium(II)

complexes bearing 2,6-substituted N,N′-di (aryl)formamidinate ligands. *Journal of the Chemical Society, Dalton Transactions*, (13), 2001–2005; (e) Cotton, F.A., Daniels, L.M., Matonic, J.H. and Murillo, C.A. (1997) Highly distorted diiron(II, II) complexes containing four amidinate ligands. A long and a short metal–metal distance. *Inorganica Chimica Acta*, **256**, 277–282.

7 Cotton, F.A., Feng, X., Matusz, M. and Poli, R. (1988) Experimental and theoretical studies of the copper(I) and silver(I) dinuclear *N,N′*-Di-p-tolylformamidinato complexes. *Journal of the American Chemical Society*, **110**, 7077–7083.

8 Pyykkö, P. and Mendizabal, F. (1998) Theory of d^{10}-d^{10} closed-shell attraction. III. Rings. *Inorganic Chemistry*, **37**, 3018–3025.

9 Laguna, A. and Laguna, M. (1999) Coordination chemistry of gold(II) complexes. *Coordination Chemistry Reviews*, **193–195**, 837–856.

10 Barker, J. and Kilner, M. (1994) The coordination chemistry of the amidine ligand. *Coordination Chemistry Reviews*, **133**, 219–300.

11 Murray, H.H., Briggs, D.A., Guillermo, Garzon, Raptis, R., Porter, L.C. and Fackler, J.P. Jr (1987) Structural characterization of a linear [Au · · · Pt · · · Au] complex, $Au_2Pt(CH_2P(S)Ph_2)_4$, and its oxidized linear metal-metal bonded [Au-Pt-Au] product, $Au_2Pt(CH_2P(S)Ph_2)_4Cl_2$. *Organometallics*, **6**, 1992.

12 Ren, T., Lin, C., Amalberti, P., Macikenas, D., Protasiewicz, J.D., Baum, J.C. and Gibson, T.L. (1998) Bis(μ-*N,N′*-η^2-*N,O*-η^2-*N′,O′*-di(o-methoxyphenyl) formamidinato)disilver(I): an interesting coordination geometry for silver(I) and room temperature fluorescence. *Inorganic Chemistry Communications*, **1**, 23–26.

13 Archibald, S.J., Alcock, N.W., Busch, D.H. and Whitcomb, D.R. (1999) Synthesis and characterization of functionalized *N,N′*-diphenylformamidinate silver(I) dimers: solid-state structures and solution properties. *Inorganic Chemistry*, **38**, 5571–5578.

14 Archibald, S.J., Alcock, N.W., Busch, D.H. and Whitcomb, D.R. (2000) Synthesis and characterization of silver(I) complexes with C-Alkyl functionalized *N,N′*-Diphenylamidinates: Tetrameric and trimeric structural motifs. *Journal of Cluster Science*, **11**, 261–283.

15 (a) Raptis, R.G., Murray, H.H. and Fackler, J.P. Jr (1987) The synthesis and crystal structure of a novel gold(I)-Pyrazolate hexamer containing an 18-Membered inorganic ring. *Journal of the Chemical Society, Chemical Communications*, (10), 737–739; (b) Murray, H.H., Raptis, R.G. and Fackler, J.P. Jr (1988) Syntheses and X-ray structures of group 11 pyrazole and pyrazolate complexes. X-ray crystal structures of Bis(3,5-diphenylpyrazole) copper(II) Dibromide, Tris(3,5-diphenylpyrazolato-*N,N′*)trisilver(I)-2-Tetrahydrofuran, Tris(3,5-diphenylpyrazolato-*N,N′*)trigold(I), and Hexakis(:-3,5-diphenylpyrazolato- *N,N′*) hexagold(I). *Inorganic Chemistry*, **27**, 26–33; (c) Raptis, R.G. and Fackler, J.P. Jr (1988) Structure of Tris(3,5-diphenylpyrazolato-*N,N′*)tricopper(I). Structural comparisons with the Silver(I) and Gold(I) pyrazolate trimers. *Inorganic Chemistry*, **27**, 4179–4182.

16 Yang, G. and Raptis, R.G. (2003) Synthesis, structure and properties of tetrameric gold(I) 3,5-di-tert-butyl–pyrazolate. *Inorganica Chimica Acta*, **352**, 98–104.

17 Irwin, M.D., Abdou, H.E., Mohamed, A.A. and Fackler, J.P. Jr (2003) Synthesis and X-ray structures of silver and gold guanidinate-like complexes. A Au(II) complex with a 2.47 Å Au-Au distance. *Chemical Communications*, (23), 2882–2883.

18 Mohamed, A.A., Mayer, A., Abdou, H.E., Irwin, M.D., Perez, L. and Fackler, J.P. Jr (2007) Dinuclear and tetranuclear gold-nitrogen complexes. Solvent influences on oxidation and nuclearity of gold

guanidinate derivatives. *Inorganic Chemistry*, **46**, 11165–11172.

19 (a) Mohamed, A.A., Abdou, H.E., Irwin, M.D., Lopez-de-Luzuriaga, J.M., and Fackler, J.P. Jr (2003) Gold(I) formamidinate clusters: The structure, luminescence, and electrochemistry of the tetranuclear. Base-free $[Au_4(ArNC(H)NAr)_4]$. *Journal of Cluster Science*, **14**, 253–266; (b) Abdou, H.E., Mohamed, A.A., López-de-Luzuriaga, J.M. and Fackler, J.P. Jr (2004) Tetranuclear gold(I) clusters with nitrogen donor ligands: luminescence and X-ray structure of gold(I) naphthyl amidinate complexes. *Journal of Cluster Science*, **15**, 397–411; (c) Abdou, H.E., Mohamed, A.A. and Fackler, J.P. Jr (2007) Synthesis, characterization, luminescence, and electrochemistry of the tetranuclear gold(I) amidinate clusters, precursors to CO oxidation catalysts: $Au_4[(ArNC(H)NAr)]_4$, $Au_4[(PhNC(Ph)NPh)]_4$ and $Au_4[PhNC(CH_3)NPh)_4]$. *Journal of Cluster Science*, **18**, 630–641; (d) Abdou, H.E., Mohamed, A.A. and Fackler, J.P. Jr (2007) Synthesis, characterization, luminescence, and electrochemistry of the tetranuclear gold(I) amidinate clusters, precursors to CO oxidation catalysts: $Au_4[(ArNC(H)NAr)]_4$, $Au_4[(PhNC(Ph)NPh)]_4$ and $Au_4[PhNC(CH_3)NPh)_4]$. *Journal of the Chinese Chemical Society*, **54**, 1107–1113.

20 Patai, S. (1975) *The Chemistry of Amidines and Imidates*, Vol. 1, John Wiley & Sons, New York.

21 Beck, J. and Strahle, J. (1986) Synthesis and structure of 1,3-Diphenyltriazenidogold (I), a tetrameric molecule with short gold-gold distances. *Angewandte Chemie (International Edition in English)*, **25**, 95–96.

22 Chiari, B., Piovesana, O., Tarantelli, T. and Zanazzi, P.F. (1985) Gold dithiocarboxylates. *Inorganic Chemistry*, **24**, 366–371.

23 Abdou, H.E., Mohamed, A.A. and Fackler, J.P. Jr (2005) Synthesis and X-ray structures of dinulear and trinuclear gold(I) and dinuclear Gold(II) amidinate complexes. *Inorganic Chemistry*, **44**, 166–168.

24 Fenske, D., Baum, G., Zinn, A. and Dehnicke, K. (1990) $Ag_2[Ph\text{-}C(NsiMe_3)_2]_2$ and $Au_2[Ph\text{-}C(NsiMe_3)_2]_2$ – amidinato complexes with short metal-metal distances. *Zeitschrift für Naturforschung B*, **45**, 1273–1278.

25 Mohamed, A.A., Kani, I., Ramirez, A.O. and Fackler, J.P. Jr (2004) Synthesis, characterization, and luminescent properties of dinuclear gold(I) xanthate complexes: X-ray structure of $[Au_2(nBu\text{-}xanthate)_2]$. *Inorganic Chemistry*, **43**, 3833–3839.

26 Van Zyl, W.E., López-de-Luzuriga, J.M., Fackler, J.P. Jr and Staples, R.J. (2001) Dithiophosphinates of Gold(I). Oxidative addition of $C1_2$ to a neutral, dinuclear gold(I) dithiophosphinate complex. X-ray crystal structures of $[AuS_2P(C_2H_5)_2]_2$, $[AuS_2PPh_2]_2$, $Au_2(CH_2)_2PMe_2(S_2PPh_2)$, and $Au_2C1_2[(CH_2)_2PMe_2][S_2PPh_2]$. *Canadian Journal of Chemistry*, **79**, 896–903.

27 King, C., Wang, J.-C., Khan, M.N.I. and Fackler, J.P. Jr (1989) Luminescence and metal-metal interactions in binuclear Gold(I) compounds. *Inorganic Chemistry*, **28**, 2145–2149.

28 (a) Van Zyl, W.E., Staples, R.J. and Fackler, J.P. Jr (1998) Dinuclear gold(I) dithiophosphonate complexes: formation, structure and reactivity. *Inorganic Chemistry Communications*, **1**, 51–54; (b) Van Zyl, W.E., Lopez-de-Luzuriaga, J.M. and Fackler, J.P. Jr (2000) Luminescence Studies of dinuclear gold(I) phosphor-1,1-dithiolate complexes. *Journal of Molecular Structure*, **516**, 99–106.

29 Herrero, G.P. and Jones, P.G. (1995) Synthesis of the first trithiocarbonatogold complex: $[N(PPh_3)_2]_2[Au_2(\mu^2\text{-}\eta^2\text{-}CS_3)_2]$. First crystal structure of a $\mu^2\text{-}\eta^2$-bridging trithiocarbonato complex. *Journal of the Chemical Society, Chemical Communications*, (7), 745–746.

30 Nazrul, Md., Khan, I., Wang, S. and Fackler, J.P. Jr (1989) Synthesis and structural characterization of $[n\text{-}Bu_4N]_2[Au_2(i\text{-}MNT)_2]$(i-MNT=1,1-Dicyanoethylene-2,2-dithiolate) and its oxidative-addition products $[Ph_4As]_2[Au_2(i\text{-}MNT)_2Cl_2]$, $[n\text{-}Bu_4N]_2[Au_2(i\text{-}MNT)_2Br_2]$, and $[n\text{-}Bu_4N][Au(i\text{-}MNT)_2]$. Spectral studies of the disproportionation of $[n\text{-}Bu_4N]_2[Au_2(i\text{-}MNT)_2X_2]$ (X=Cl-, Br-, I-) into $[n\text{-}Bu_4N][AuX_2]$ and $[n\text{-}Bu_4N][Au(i\text{-}MNT)_2]$. *Inorganic Chemistry*, **28**, 3579–3588.

31 Mansour, M.A., Connick, W.B., Lachicotte, R.J., Gysling, H.J. and Eisenberg, R. (1998) Linear chain Au(I) dimer compounds as environmental sensors: A luminescent switch for the detection of volatile organic compounds. *Journal of the American Chemical Society*, **120**, 1329–1330.

32 Fackler, J.P. (1997) Polyhedron report No. 63, metal-metal bond formation in the oxidative addition to dinuclear Gold(I) species. Implications from dinuclear and trinuclear gold chemistry for the oxidative addition process generally. *Polyhedron*, **16**, 1–17.

33 Abdou, H.E., Mohamed, A.A. and Fackler, J.P. Jr (2004) Oxidative addition of methyl iodide to dinuclear Gold(I) amidinate complex: schmidbaur's breakthrough reaction revisited with amidinates. *Zeitschrift für Naturforschung B. A Journal of Chemical Sciences*, **59**, 1480–1482.

34 Abdou, H.E., Mohamed, A.A. and Fackler, J.P. Jr (2007) Oxidative-addition to the dinuclear Au(I) amidinate complex, $[Au_2(2,6\text{-}(CH_3)_2Ph\text{-}form)_2]$. Syntheses and characterization of the Au(II) amidinate complexes. The first dinuclear Gold(II) nitrogen complex possessing bonds to oxygen. *Inorganic Chemistry*, **46**, 9692–9699.

35 Porter, L.C. and Fackler, J.P. Jr (1986) Structure of the first example of an organometallic dinuclear gold(II) complex possessing bonds to oxygen. *Acta Crystallographica*, **42**, 1128–1131.

36 Mohamed, A.A., Abdou, H.E. and Fackler, J.P. Jr (2006) Mercury(II) cyanide coordination polymer with dinuclear gold (I) amidinate. Structure of the 2-D $[Au_2(2,6\text{-}Me_2\text{-}formamidinate)_2]\cdot 2Hg(CN)_2\cdot 2THF$ complex. *Inorganic Chemistry*, **45**, 11–12.

37 Murray, H.H., Mazany, A.M. and Fackler, J.P. Jr (1985) Molecular structures of $[Au(CH_2)_2PPh_2]_2(CN)_2$ and $[(CH_2)Au(CH_2)_2PPh_2]_2(CN)_2$. The first ylide dimer possessing Gold(III) centers bonded only to carbon. *Organometallics*, **4**, 154–157.

38 Mohamed, A.A., Bruce, A.E. and Bruce, M.R.M. (1999) The electrochemistry of gold and silver complexes, in *Chemistry of Organic Derivatives of Gold and Silver* (ed. S. Patai), John Wiley and Sons, New York.

39 Abdou, H. (2006) PhD. Thesis New Chemistry with Gold-Nitrogen Complexes: Synthesis and Characterization of Tetra-, Tri-, and Dinuclear Gold(I) Amidinate Complexes. Oxidative-Addition to the Dinuclear Gold (I) Amidinate, A&M University, Texas.

40 Abdou, H.E., Mohamed, A.A. and Fackler, J.P. Jr (2007) Syntheses of mixed-ligand tetranuclear Gold(I)-Nitrogen clusters by ligand exchange reactions with the dinuclear Gold(I) formamidinate complex $Au_2(2,6\text{-}Me_2Ph\text{-}form)_2$. *Inorganic Chemistry*, **46**, 141–146.

41 (a) Cotton, F.A., Gruhn, N.E., Gu, J., Huang, P., Lichtenberger, D.L., Murillo, C.A., Van Dorn, L.O. and Wilkinson, C.C. (2002) Most easily-ionized, closed-shell molecules known; easier than the cesium atom. *Science*, **298**, 1971–1974; (b) Wilkinson, Chad (2005) PhD. Thesis, A&M University, Texas; (c) Soria, D.B., Grundy, J., Coles, M.P. and Hitchcock, P.B. (2005) Stabilisation of high oxidation-state niobium using "electron-rich" bicyclic-guanidinates. *Journal of Organometallic Chemistry*, **690**, 2278–2284; (d) Cotton, F.A., Durivage, J.C., Gruhn Lichtenberger, D.L., Murillo, C.A., Van, L.O. and Wilkinson, C.W. (2006) Photoelectron

spectroscopy and DFT calculations of easily ionized quadruply bonded $Mo_2$4 + compounds and their bicyclic guanidinate precursors. *The Journal of Physical Chemistry B*, **110**, 19793–19798.

42 Cotton, F.A., Feng, X. and Timmons, D.J. (1998) Further study of very close non-bonded Cu^{I}–Cu^{I} contacts. molecular structure of a new compound and density functional theory calculations. *Inorganic Chemistry*, **37**, 4066–4069.

43 Burini, A., Mohamed, A. and Fackler, J.P. (2003) Cyclic trinuclear Gold(I) compounds: synthesis. structures and supramolecular acid-base π-stacks. *Comments on Inorganic Chemistry*, **24**, 253–280.

44 Vaughan, L.G. (1970) Organogold chemistry. III. 2-Pyridylgold(I). *Journal of the American Chemical Society*, **11**, 730–731.

45 Hayashi, A., Olmstead, M.M., Attar, S. and Balch, A.L. (2002) Crystal chemistry of the Gold (I) trimer, $Au_3(NC_5H_4)_3$: formation of hourglass figures and self-association through aurophilic attraction. *Journal of the American Chemical Society*, **124**, 5791–5795.

46 Bonati, F. and Minghetti, G. (1972) Trimeric 1-(Cyclohexylimino) methoxymethylgold(I), A new type of organometallic compound. *Angewandte Chemie International Edition*, **11**, 429.

47 Parks, J.E. and Balch, A.L. (1974) Gold carbene complexes: preparation, oxidation, and ligand displacement. *Journal of Organometallic Chemistry*, **71**, 453–463.

48 (a) Vickery, J.C., Olmstead, M.M., Fung, E.Y. and Balch, A.L. (1997) Solvent-stimulated luminescence from the supramolecular aggregation of a trinuclear Gold(I) complex that displays extensive intermolecular Au · · · Au interactions. *Angewandte Chemie (International Edition in English)*, **36**, 1179–1181; (b) Vickery, J.C., Olmstead, M.M., Fung, E.Y. and Balch, A.L. (1998) Glowing gold rings: solvoluminescence from planar trigold(I) complexes. *Coordination Chemistry Reviews*, **171**, 151–159; (c) Gade, L.H. (1997) "Hyt was of Gold, and Shon so Bryghte. . .": Luminescent Gold(I) Compounds. *Angewandte Chemie (International Edition in English)*, **36**, 1171–1173.

49 Minghetti, G. and Bonati, F. (1974) Trimeric (alkoxy)(alkylimino)methylgold(I) compounds, $[(RO)(R'N{=})CAu]_3$. *Inorganic Chemistry*, **13**, 1600–1602.

50 Tiripicchio, A., Tiripicchio Camellini, M. and Minghetti, G. (1979) The crystal structure of tris-μ-[(ethoxy)(*N-p*-tolylimino)methyl-*N, C*]trigold(I), $[(EtO)(MeC_6H_4N{=})CAu]_3$. *Journal of Organometallic Chemistry*, **171**, 399–406.

51 Bonati, F., Burini, A., Pietroni, B.R. and Bovio, B. (1989) Reactions of *C*-imidazolyllithium derivatives with Group Ib compounds: Tris[μ-(1-alkylimidazolato-N^3,C^2)]tri-gold(I) and -silver(I). Crystal structure of bis (1-benzylimidazolin-2-yliden)gold(I) chloride. *Journal of Organometallic Chemistry*, **375**, 147–160.

52 Bonati, F., Burini, A., Pietroni, B.R. and Galassi, R. (1993) Gold(I) Derivatives of Furan, Thiophene, 2-mercaptopyridine, and of some Pyrazoles – Mass-spectroscopic evidence of tetranuclear Gold(I) compounds. *Gazzetta Chimica Italiana*, **123**, 691.

53 Banditelli, G., Bandini, A.L., Bonati, F. and Goel, R.G. (1982) Some New Gold(I) complexes with bulky ligands. *Gazzetta Chimica Italiana*, **112**, 539.

54 Bovio, B., Bonati, F. and Banditelli, G. (1984) X-ray crystal structure of tris[μ-3,5-bis(trifluoromethyl)pyrazolato-*N,N'*] trigold(I), a compound containing an inorganic nine-membered ring. *Inorganica Chimica Acta*, **87**, 25–33.

55 Barberà, J., Elduque, A., Gimenez, R., Oro, L.A. and Serrano, J.L. (1996) Pyrazolate Golden Rings: trinuclear complexes that form columnar mesophases at room temperature. *Angewandte Chemie (International Edition in English)*, **35**, 2832–2836.

56 Barberà, J., Elduque, A., Gimenez, R., Lahoz, F.J., Oro, L.A. and Serrano, J.L. (1998) (Pyrazolato)gold complexes showing room-temperature columnar mesophases. Synthesis, properties, and structural characterization. *Inorganic Chemistry*, **37**, 2960–2967.

57 Yang, G. and Raptis, R.G. (2003) Supramolecular assembly of trimeric Gold(I) pyrazolates through aurophilic attractions. *Inorganic Chemistry*, **42**, 261–263.

58 (a) Balch, A.L. and Doonan, D.J. (1977) Mixed valence gold chemistry: Stepwise oxidation of a cyclic trigold(I) complex. *Journal of Organometallic Chemistry*, **131**, 137; (b) Minghetti, G., Banditelli, G. and Bonati, F. (1979) Metal derivatives of azoles. 3. The pyrazolato anion (and homologs) as a mono- or bidentate ligand: preparation and reactivity of tri-, bi-, and mononuclear gold(I) derivatives. *Inorganic Chemistry*, **18**, 658–663; (c) Raptis, R.G. and Fackler, J.P. Jr (1990) Synthesis and crystal structure of a mixed-valence, AuI-AuIII, pyrazolato complex stable in aqua regia. X-ray photoelectron study of homo- and heterovalent gold-pyrazolato trimers. *Inorganic Chemistry*, **29**, 5003; (d) Bonati, F., Burini, A., Pietroni, B.R. and Bovio, B. (1991) Reactions of symmetric *C*-imidazolylgold(I) leading to Au^{I} carbene complexes or mixed valence or Au^{III} imidazolyl derivatives. Crystal structure of [1-benzyl-3-(carboethoxy)imidazolin-2-yliden]chlorogold(I). *Journal of Organometallic Chemistry*, **408**, 271–280; (e) Raptis, R.G., Murray, H.H. and Fackler, J.P. Jr (1988) The structure of $[Au\{3,5\text{-}(C_6H_5)_2C_3HN_2\}]_3Cl_2$: a trinuclear mixed-valence gold pyrazolate complex. *Acta Crystallographica Section C: Crystal Structure Communications*, **44**, 970; (f) Bovio, B., Burini, A. and Pietroni, B.R. (1993) Reactions of trimeric 1-benzyl-2-gold(I)imidazole leading to Au^{I} carbene complexes. Crystal structure of [1-benzyl-3-benzoyl-imidazolin-2-yliden]chlorogold (I). *Journal of Organometallic Chemistry*, **452**, 287–291; (g) Vickery, J.C. and Balch, A.L. (1997) X-ray crystallographic studies of the products of oxidative additions of iodine to cyclic trinuclear Gold(I) complexes: directional effects for Au-I···I-Au interactions. *Inorganic Chemistry*, **36**, 5978–5983.

59 Burini, A., Pietroni, B.R., Bovio, B., Calogero, S. and Wagner, F.E. (1994) A ^{197}Au mössbauer study of reaction products of trimeric 1-benzyl-2-gold(I)-imidazole leading to Au^{I} carbene or Au^{I} imidazoline complexes and trinuclear Au^{III} imidazolyl derivatives. X-Ray crystal structure of $[\{(\mu\text{-}1\text{-benzylimidazolato-}N^3, C^2)Au\}_3I_2]$. *Journal of Organometallic Chemistry*, **470**, 275–283.

60 Miller, J.S. (ed.) (1982) *Extended Linear Chain Compounds*, Vol. 1–3, Plenum Press, New York.

61 Hoffmann, R. (1987) How chemistry and physics meet in the solid state. *Angewandte Chemie (International Edition in English)*, **26**, 846–878.

62 Kunugi, Y., Mann, K.R., Miller, L.L. and Exstrom, C.L. (1998) A vapochromic LED. *Journal of the American Chemical Society*, **120**, 589–590.

63 (a) Fernández, E.J., López-de-Luzuriaga, J.M., Monge, M., Olmos, M.E., Pérez, J., Laguna, A., Mohamed, A.A. and Fackler, John P. Jr (2003) $\{Tl[Au(C_6Cl_5)_2]\}_n$: A vapochromic complex. *Journal of the American Chemical Society*, **125**, 2022–2023; (b) Fernández, E.J., López-de-Luzuriaga, J.M., Monge, M., Olmos, M.E., Pérez, J., Laguna, A., Mohamed, A.A. and Fackler, John P. Jr (2004) A Detailed study of the vapochromic behavior of $\{Tl[Au(C_6Cl_5)_2]\}_n$. *Inorganic Chemistry*, **43**, 3573–3581; (c) Fernández, E.J., Laguna, A., López-de-Luzuriaga, J.M., Monge, M., Montiel, M., Olmos, M.E. and Rodríguez-Castillo, M. (2006) Mesitylgold(I) and silver(I) perfluorocarboxylates as precursors of supramolecular Au/Ag systems. *Organometallics*, **25**, 4307–4315.

64 Burini, A., Fackler, J.P. Jr, Galassi, R., Grant, T.A., Omary, M.A.,

Rawashdeh-Omary, M.A., Pietroni, B.R. and Staples, R.J. (2000) Supramolecular chain assemblies formed by interaction of a B molecular acid complex of mercury with B-Base trinuclear gold complexes. *Journal of the American Chemical Society*, **122**, 11264.

65 Rawashdeh-Omary, M.A., Omary, M.A., Fackler, J.P. Jr, Galassi, R., Pietroni, B.R. and Burini, A. (2001) Chemistry and optoelectronic properties of stacked supramolecular entities of trinuclear Gold(I) complexes sandwiching small organic acids. *Journal of the American Chemical Society*, **123**, 9689.

66 (a) Mohamed, A.A., Manal, A., Rawashdeh-Omary, M.A., Omary, M.A. and Fackler, J.P. Jr (2005) External heavy-atom effect of gold in a supramolecular acid-base pi stack. *Dalton Transactions*, (15), 2597; (b) Omary, M.A., Mohamed, A.A., Rawashdeh-Omary, M.A. and Fackler, J.P. Jr (2005) Photophysics of supramolecular binary stacks consisting of electron-rich trinuclear Au(I) and organic electrophiles Coord. *Chemical Reviews*, **249**, 1372.

67 Olmstead, M.M., Jiang, F., Attar, S. and Balch, A.L. (2001) Alteration of the aurophilic interactions in trimeric Gold(I) compounds through charge transfer. behavior of solvoluminescent $Au_3(MeN{=}COMe)_3$ in the presence of electron acceptors. *Journal of the American Chemical Society*, **123**, 3260.

68 Gabbaï, F.P., Schier, A., Riede, J. and Tschinkl, M.T. (1999) Micropore decoration with bidentate lewis acids: spontaneous assembly of 1,2-Bis(chloromercurio) tetrafluorobenzene. *Angewandte Chemie International Edition*, **38**, 3547.

69 Tsunoda, M. and Gabbaï, F.P. (2000) μ_6-η^2:η^2:η^2:η^2:η^2:η^2 As a new bonding mode for benzene. *Journal of the American Chemical Society*, **122**, 8335–8336.

70 Burini, A., Fackler, J.P. Jr, Galassi, R., Macchioni, A., Omary, M.A., Rawashdeh, M.A.-O., Pietroni, B.R., Sabatini, S. and Zuccaccia, C. (2002) ^{19}F, ^{1}H-HOESY and PGSE NMR studies of neutral trinuclear complexes of Au1 and HgII: evidence for acid-base stacking in solution. *Journal of the American Chemical Society*, **124**, 4570.

71 (a) Teo, B.K. and Keating, K. (1984) Novel triicosahedral structure of the largest metal alloy cluster: hexachlorododecakis (triphenylphosphine)-gold-silver cluster $[(Ph_3P)_{12}Au_{13}Ag_{12}Cl_6]m+$. *Journal of the American Chemical Society*, **106**, 2224; (b) Teo, B.K., Zhang, H. and Shi, X. (1990) Molecular architecture of a novel vertex-sharing biicosahedral cluster $[(p\text{-}Tol_3P)_{10}Au_{13}Ag_{12}Br_8](PF_6)$ containing a staggered-staggered-staggered configuration for the 25-atom metal framework. *Inorganic Chemistry*, **29**, 2083–2091; (c) Teo, B.K., Shi, X. and Zhang, H. (1991) Cluster of clusters. Structure of a novel gold-silver cluster $[(Ph_3P)_{10}Au_{13}Ag_{12}Br_8](SbF_6)$ containing an exact staggered-eclipsed-staggered metal configuration. Evidence of icosahedral units as building blocks. *Journal of the American Chemical Society*, **113**, 4329–4331; (d) Teo, B.K. and Zhang, H. (1991) Cluster of clusters. Structure of a new cluster $[(p\text{-}Tol_3P)_{10}Au_{13}Ag_{12}Cl_7](SbF_6)_2$ containing a nearly staggered-eclipsed-staggered metal configuration and five doubly-bridging ligands. *Inorganic Chemistry*, **30**, 3115–3116; (e) Teo, B.K. and Zhang, H. (1992) Molecular machines: molecular structure of $[(p\text{-}Tol_3P)_{10}Au_{13}Ag_{12}Cl_8](PF_7)$ – a Cluster with a biicosahedral rotorlike metal core and an unusual arrangement of bridging ligands. *Angewandte Chemie (International Edition in English)*, **31**, 445–447; (f) Teo, B.K., Shi, X. and Zhang, H. (1992) Cluster rotamerism of a 25-metal-atom cluster $[(Ph_3P)_{10}Au_{13}Ag_{12}Br_8]^+$ monocation: a molecular rotary unit. *Journal of the Chemical Society, Chemical Communications*, (17), 1195–1196; (g) Teo, B.K., Dang, H., Campana, C.F. and Zhang, H. (1998) Synthesis, structure, and

charactreization of $(MePh_2P)_{10}Au_{12}Ag_{13}Br_9$: The first example of a neutral bi-icosahedral Au···Ag cluster with a novel seven-membered satellite ring of bridging ligands. *Polyhedron*, **17**, 617–621; (h) Usón, R., Laguna, A., Laguna, M., Manzano, B.R., Jones, P.G. and Sheldrick, G.M. (1984) Synthesis and reactivity of bimetallic Au–Ag polyfluorophenyl complexes; crystal and molecular structures of $[\{AuAg(C_6F_5)_2(SC_4H_8)\}_n]$ and $[\{AuAg(C_6F_5)_2(C_6H_6)\}_n]$. *Journal of the Chemical Society, Dalton Transactions*, (2), 285; (i) Usón, R., Laguna, A., Laguna, M., Usón, R., Laguna, A., Laguna, M., Jones, P.G. and Erdbrügger, C.F. (1987) Bimetallic phosphorus ylide gold-silver complexes. *Organometallics*, **6**, 1778–1780; (j) Tran, N.T., Powell, D.R. and Dahl, L.F. (2004) Generation of $AuPd_{22}/Au_2Pd_{21}$ analogues of the high-nuclearity $Pd_{23}(CO)_{20}(PEt_3)_{10}$ cluster containing 19-atom centered hexacapped-cuboctahedral (ν_2-octahedral) metal fragment: structural-to-synthesis approach concerning formation of $Au_2Pd_{21}(CO)_{20}(PEt_3)_{10}$. *Dalton Transactions*, (2), 209–216; (k) Tran, N.T., Powell, D.R. and Dahl, L.F. (2004) Nanosized $Au_2Pd_{41}(CO)_{27}(PEt_3)_{15}$ containing two geometrically unprecedented 13-coordinated Au-centered $(\mu_{13}\text{-Au})Pd_{13}$ polyhedra connected by triangular face-sharing and three interpenetrating 12-coordinated Pd-centered $(\mu_{12}\text{-Pd})Au_2Pd_{10}$ icosahedra: geometrical change in centered polyhedra induced by Au/Pd electronegativity-mismatch. *Dalton Transactions*, (2), 217–223; (l) Catalano, V.J. and Horner, S.J. (2003) Luminescent Gold(I) and Silver(I) Complexes of 2-(Diphenylphosphino)-1-methylimidazole (dpim): Characterization of a Three-Coordinate Au(I)-Ag(I) Dimer with a Short Metal-Metal Separation. *Inorganic Chemistry*, **42**, 8430–8438; (m) Rawashdeh-Omary, M.A., Omary, M.A. and Fackler, J.P. Jr (2002) Argento-aurophilic Bonding in Organosulfur Complexes. The Molecular and Electronic Structures of the Heterobimetallic Complex $AgAu(MTP)_2$. *Inorganica Chimica Acta*, **334**, 376.

72 (a) Rousset, J.L., Aires, J.C.S., Sekhar, R., Mélinon, P., Prevel, B. and Pellarin, M. (2000) Comparative X-ray photoemission spectroscopy study of Au, Ni, and AuNi clusters produced by laser vaporization of bulk metals. *The Journal of Physical Chemistry B*, **104**, 5430–5435; (b) Rainer, D.R., Xu, C., Holmblad, P.M. and Goodman, D.W. (1997) Pd, Cu, and Au particles on Al_2O_3 thin films: An infrared reflection absorption spectroscopy study of monometallic and bimetallic planar model supported catalysts. *Journal of Vacuum Science & Technology A, Vacuum Surfaces and Films*, **15**, 1653–1662; (c) Baddeley, C.J., Tikhov, M., Hardacre, C., Lomas, J.R. and Lambert, R.M. (1996) Ensemble effects in the coupling of acetylene to benzene on a bimetallic surface: A study with Pd{111}/Au. *The Journal of Physical Chemistry*, **100**, 2189–2194; (d) Reifsnyder, S.N. and Lamb, H.H. (1999) Characterization of silica-supported Pd-Au clusters by X-ray absorption spectroscopy. *The Journal of Physical Chemistry B*, **103**, 321–329.

73 (a) Andres, R.P., Bein, T., Dorogi, M., Feng, S., Henderson, J.I., Kubiak, C.P., Mahoney, W., Osifchin, R.G. and Reifenberger, R. (1996) "Coulomb Staircase" at Room Temperature in a Self-Assembled Molecular Nanostructure. *Science*, **272**, 1323–1325; (b) Mirkin, C.A., Letsinger, R.L., Mucic, R.C. and Storhoff, J.J. (1996) A DNA-based method for rationally assembling nanoparticles into macroscopic materials. *Nature*, **382**, 607–609; (c) Alivisatos, A.P., Johnson, K.P., Peng, X., Wilson, T.E., Loweth, C.J., Bruchez, M.P. Jr and Schultz, P.G. (1996) Organization of 'nanocrystal molecules' using DNA. *Nature*, **382**, 609–611; (d) Hong, B.H., Bae, S.C., Lee, C.W., Jeong, S. and Kim, K.S. (2001) Ultrathin single-crystalline silver nanowire arrays formed in an ambient solution phase. *Science*, **294**,

348–351; (e) Hong, B.H., Lee, J.Y., Lee, C.W., Kim, J.C., Bae, S.C. and Kim, K.S. (2001) Self-assembled arrays of organic nanotubes with infinitely long one-dimensional H-Bond chains. *Journal of the American Chemical Society*, **123**, 10748–10749.

74 (a) Mohamed, A.A., Burini, A. and Fackler, J.P. Jr (2005) Mixed-metal triangular trinuclear complexes: dimers of gold-silver mixed-metal complexes from Gold(I) carbenieates and Silver(I) 3,5-Diphenylpyrazolates. *Journal of the American Chemical Society*, **127**, 5012; (b) Mohamed, A.A., Galassi, R., Fabrizio, P., Burini, A. and Fackler, J.P. Jr (2006) Gold(I) and Silver(I) mixed-metal trinuclaer complexes: dimeric products from the reaction of Gold(I) carbeniates or benzylimidazolates with Silver(I) 3,5-Diphenylpyrazolate. *Inorganic Chemistry*, **45**, 7770–7776.

75 Mohamed, A.A., Perez, L.M. and Fackler, J.P. Jr (2005) Unsupported intermolecular argentophilic interaction in the dimer of trinuclear silver(I) 3,5-diphenylpyrazolates. *Inorganica Chimica Acta*, **358**, 1657–1662.

76 (a) Yan, Z., Chinta, S., Mohamed, A.A., Fackler, J.P. Jr and Goodman, D.W. (2005) The role of F-centers in catalysis by Au supported on MgO. *Journal of the American Chemical Society*, **127**, 1604–1605; (b) Yan, Z., Chinta, S., Mohamed, A.A., Fackler, J.P. Jr and Goodman, D.W. (2006) CO Oxidation over Au/TiO2 prepared from metal-organic gold complexes. *Catalysis Letters*, **111**, 15–18.

77 Guzman, J. and Gates, B.C. (2003) Structure and reactivity of a mononuclear gold-complex catalyst supported on magnesium oxide. *Angewandte Chemie International Edition*, **42**, 690–693.

78 Oh, H.-S., Yang, J.H., Costello, C.K., Wang, Y.M., Bare, S.R., Kung, H.H. and Kung, M.C. (2002) Selective catalytic oxidation of CO: Effect of chloride on supported au catalysts. *Journal of Catalysis*, **210**, 375–386.

79 Broqvist, P., Molina, L.M., Grönbecka, H. and Hammer, B. (2004) Promoting and poisoning effects of Na and Cl coadsorption on CO oxidation over MgO-supported Au nanoparticles. *Journal of Catalysis*, **227**, 217–226.

80 Sladek, A., Hofreiter, S., Paul, M. and Schmidbaur, H. (1995) Sodium tetraphenylborate as a phenylating agent for gold(I) complexes. *Journal of Organometallic Chemistry*, **501**, 47–51.

81 Forward, J.M., Fackler, J.P. and Staples, R.J. (1995) Synthesis and structural characterization of the luminescent Gold(I) Complex $[(MeTPA)_3AuI]I_3$. Use of $NaBPh_4$ as a phenyl transfer reagent to form $[(MeTPA)AuPh](BPh_4)$ and (TPA) AuPh. *Organometallics*, **14**, 4194–4198.

82 Partyka, D.V., Zeller, M., Hunter, A.D. and Gray, T.G. (2006) Relativistic functional groups: Aryl carbon-gold bond formation by selective transmetalation of boronic acids. *Angewandte Chemie International Edition*, **45**, 8188–8191.

83 There are several recent reviews: (a) Hashmi, A.S.K. (2007) Gold-catalyzed organic reactions. *Chemical Reviews*, **107**, 3180–3211; (b) Gorin, D.J. and Toste, D.F. (2007) Relativistic effects in homogeneous gold catalysis. *Nature*, **446**, 395–403; (c) Hashmi, A.S.K. and Hutchings, G.J. (2006) Gold Catalysis. *Angewandte Chemie International Edition*, **45**, 7896–7936.

84 Gray, T.G. (2007) Gilded organometallics. *Comments on Inorganic Chemistry*, **28**, 181–212.